Soil carbon sequestration and CO_2 flux partitioning

Isotopic patterns, models, applications

Dissertation

zur Erlangung des akademischen Grades doctor rerum naturalium

(Dr. rer. nat.)

vorgelegt dem Rat der Chemisch-Geowissenschaftlichen Fakultät

der Friedrich-Schiller-Universität Jena

von Volker Hahn, geboren am 4. Mai 1974 in Bielefeld

Gutachter:

1.

2.

3.

Table of contents

1 Introduction 1

2 Modeling the amount and turnover of active soil organic carbon 4

2.1 Introduction 4

2.2 Methods 5

2.3 Results 12

2.4 Discussion 18

3 Separating heterotrophic and autotrophic soil respiration 21

3.1 Introduction 21

3.2 Methods 23

3.3 Results 29

3.4 Discussion 33

4 Isotopic composition of soil CO_2 and soil respired CO_2 in European forests along a latitudinal and two age gradients 36

4.1 Introduction 36

4.2 Methods 38

4.3 Results 40

4.4 Discussion 52

5 Concluding discussion 57

6 Abstract 61

7 References 64

8 Acknowledgements 74

9 Appendix 75

1 Introduction

Fossil fuel burning, cement production and land-use change have caused an increase of atmospheric CO_2 mixing ratios from approximately 280 ppm at pre-industrial level to approximately 370 ppm today. This rise in atmospheric CO_2 is believed to be one of the major causes for global warming (IPCC 2001). Independent atmospheric and land-based approaches estimate that the terrestrial biosphere sequesters carbon and thereby reduces the amount of CO_2 in the atmosphere. However, the uncertainties are large. E.g., it is unclear whether Europe´s terrestrial ecosystems are a net carbon sink or source (Janssens et al. 2003a).

Soil organic carbon (SOC) is the largest carbon pool in terrestrial ecosystems that is in close exchange with the atmosphere. At least twice as much carbon is stored in SOC as in the atmosphere (Jobbagy and Jackson 2000, Schlesinger 1997). Changes in the amounts of SOC can therefore significantly alter mixing ratios of atmospheric CO_2. Carbon enters the SOC pool as litter (above- and below-ground) and is returned to the atmosphere by decomposition (heterotrophic respiration). There is an ongoing debate, if carbon inputs into SOC exceed carbon losses through heterotrophic respiration, resulting in growing SOC pools and net soil carbon sequestration (e.g., Gill et al. 2002, Hagedorn et al. 2003, Poulton et al. 2003, Schlesinger and Lichter 2001, Schulze et al. 2000, Sleutel et al. 2003, Telles et al. 2003). Key variables for assessing carbon sequestration potential of soils are the amounts of SOC and the rates at which this SOC is turned over. Of particular interest are the environmental factors controlling amount and turnover of SOC and the potential effects of changes in climate or management on soil carbon sequestration.

For modeling SOC turnover, carbon isotopes have proven a useful tool. The shift in the ^{13}C content of SOC after a C3/C4 vegetation change has been frequently used to model SOC turnover (e.g., Gleixner et al. 2002, Krull and Skjemstad 2003, Magid et al. 2002, Powers and Schlesinger 2002). Where no vegetation change occurred, ^{14}C (radiocarbon) is an alternative tracer. ^{14}C is continuously produced in the atmosphere by the reaction of secondary neutrons (naturally produced by the interaction of cosmic radiation and atomic nuclei) and ^{14}N. The freshly produced ^{14}C is subsequently oxidized to ^{14}CO and $^{14}CO_2$. The ^{14}C content of atmospheric CO_2 remained at a fairly stable level, before it rapidly increased after nuclear bomb tests in the fifties and sixties (Figure 1). As a result of the treaty against such tests, the ^{14}C content of atmospheric CO_2 is continuously decreasing since 1963, due to fossil fuel burning and carbon exchange with oceanic and terrestrial ecosystems. Through photo-

synthesis and litter, the ^{14}C enriched atmospheric carbon ("bomb carbon") has entered and labeled SOC. ^{14}C models make use of annually changing ^{14}C contents of litter to calculate the turnover of SOC fractions (e.g., Gaudinski et al. 2000, Harkness et al. 1986, Harrison et al. 2000, Hsieh 1993, O'Brien and Stout 1978, Trumbore et al. 1989, Trumbore et al. 1996, Wang et al. 1996). However, all available ^{14}C turnover models have major deficiencies in constraining the true ^{14}C content of carbon entering and leaving the respective fractions of SOC. Thus, in this study, a new ^{14}C model was developed that overcomes these major deficiencies. This so called "two-pool model" is presented in chapter 2. The new model can be used to calculate the turnover time of a model-defined active carbon pool and additionally yields the amount of carbon in this pool. Applying the new model, the first major challenge of this study was addressed, namely to determine turnover times and amounts of active soil carbon for a variety of forest stands in Europe and to assess the potential of soils for carbon sequestration. Additionally, I aimed at constraining potential factors controlling amounts and turnover of active soil carbon, such as climate and stand age, and to assess potential effects of environmental changes on soil carbon dynamics.

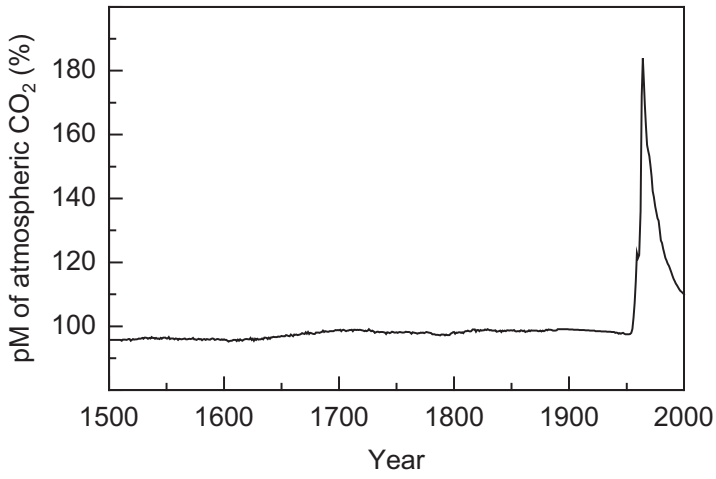

Figure 1. pM (percent Modern) of atmospheric CO_2 during the last 500 years. pM is a relative measure of the ^{14}C content.

Soil respiration is one of the most important processes causing carbon loss from soils (SOC and roots) and controlling ecosystem carbon sequestration (Schlesinger 1997). A major uncertainty in our understanding of the terrestrial carbon cycle is how soil respiration is divided between heterotrophic respiration (respiration by saprotrophic fungi, microbes and animals) on the one hand and autotrophic respiration (respiration by plant roots and their associated mycorrhiza) on the other hand. The separation of these two fluxes is essential for assessing the individual responses of both processes to environmental factors and to potential

changes in climate or management. However, available methods for the partitioning of autotrophic and heterotrophic respiration are either destructive or only applicable to a small number of ecosystems (Hanson et al. 2000).

Heterotrophically respired CO_2 has been reported to be enriched in ^{14}C compared to autotrophically respired CO_2 (Certini et al. 2003, Wang et al. 2000). Therefore, heterotrophic and autotrophic soil respiration could be separated, if the ^{14}C contents of CO_2 originating from the two processes could be determined. Since roots respire recently assimilated carbon (Ekblad and Högberg 2001, Högberg et al. 2001, Horwath et al. 1994), autotrophically respired CO_2 should have the same ^{14}C content as current atmospheric CO_2 (Dörr and Münnich 1986, Wang et al. 2000), which can be measured. Furthermore, the ^{14}C content of total heterotrophically respired CO_2 could be estimated using ^{14}C models like the two-pool model presented in chapter 2. Until now, models have not been used in such a way. Thus, the second major challenge of this study was to develop and validate a new approach for partitioning heterotrophic and autotrophic soil respiration using ^{14}C models (chapter 3) and to determine heterotrophic and autotrophic respiration rates for a variety of European forest stands (chapter 4).

In addition to these major challenges, spatial and temporal patterns of the ^{13}C, ^{14}C and ^{18}O contents of soil CO_2 and soil respired CO_2 were investigated for a selection of European forests stands along a latitudinal gradient and two age gradients (chapter 4). The aim was to elucidate factors controlling the isotopic composition of soil CO_2 and soil respired CO_2.

In chapter 5, the major results of chapters 2 to 4 are resumed and discussed, and the achievements of this study for carbon cycle research are evaluated. Finally, a perspective is provided for potential future research activities, using the newly developed model and the new partitioning approach, for further improvement of our understanding of soil and ecosystem carbon dynamics.

2 Modeling the amount and turnover of active soil organic carbon

2.1 Introduction

One of the key variables to assess current and future potential of soils to sequester and store carbon is the turnover of soil organic carbon.

Scientists have developed and applied models that use bomb carbon (^{14}C enrichment) as a tracer to calculate the turnover of SOC (e.g., Gaudinski et al. 2000, Harkness et al. 1986, Harrison et al. 2000, Hsieh 1993, O'Brien and Stout 1978, Trumbore et al. 1989, Trumbore et al. 1996, Wang et al. 1996). The high potential of these ^{14}C models to calculate SOC turnover rates has been reviewed recently by Wang and Hsieh (2002). But ^{14}C models still have two major deficiencies: (1) In most models, the input of carbon into different soil depths or SOC fractions has a ^{14}C content that corresponds to current atmospheric ^{14}C. However, this is not always true, as also old carbon (having a very different ^{14}C content) is transferred within the soil profile into new depths or new SOC fractions. (2) The models assume that respired CO_2 has the same ^{14}C content as the SOC or SOC fraction it originates from. Especially if unfractionated soil is used for ^{14}C determinations, this seems unrealistic, as particularly the mineral soil has accumulated recalcitrant, “background” carbon over time, which hardly contributes to soil respiration (Trumbore and Zheng 1996, Wang and Hsieh 2002).

Here, a new ^{14}C model for calculating the turnover time of active soil organic carbon is presented. Additionally, the model calculates the amount and ^{14}C content of this active carbon pool. The aim was to overcome the major deficiencies of older ^{14}C models and to validate the model performance. The model was applied to 25 European forest stands. I determined relationships of active carbon amount and turnover time with environmental and stand variables, such as climate and stand age. Finally, the carbon sequestration potential of soils is assessed.

2.2 Methods

2.2.1 Model explanation

For this new model, the top soil SOC pool is divided into two subpools, the passive pool (PP) and the active pool (AP). Therefore, the model is called the "two-pool model". The passive pool is assigned a pM (percent Modern) value of

$$pM_{PP} = 97.5\,\%, \tag{1}$$

with

$$pM = \frac{A \times \left(\frac{975}{1000 + \delta^{13}C} \right)^2}{A_{ON}} \times 100\,\%, \tag{2}$$

where A is the ^{14}C activity of the sample, A_{ON} is the ^{14}C activity of the standard normalized for ^{13}C fractionation, and $\delta^{13}C$ is the $\delta^{13}C$ value of the sample (Rom et al. 2000). This definition of pM is used by several AMS laboratories (Vienna, Kiel, Oxford) and corresponds to $^{14}a_N$ as defined by Mook and van der Plicht (1999). Note that the pM value of an individual substance, e.g., a sample of SOC or leaves, does not change with time, as both sample and standard are subject to the same radioactive decay. pM also accounts for kinetic fractionation and remains thus unchanged by photosynthesis.

The assigned value of pM_{PP} equals the mean pM value of atmospheric CO_2 from 1500 to 1950 (Figure 1). Note that during these 450 years, pM of atmospheric CO_2 stayed very constant. In the two-pool model, it is assumed that carbon contributions to the passive pool from before 1500 (pM < 97.5%) and from after 1950 (pM > 97.5%) are minor and can therefore be neglected.

The mixture of both the passive pool and the active pool forms the top soil carbon pool. Here, top soil is defined as all SOC with pM > 97.5%, i.e., SOC containing bomb carbon. The size of the passive pool is defined as

$$C_{PP} = C_{top} - C_{AP}, \tag{3}$$

with C_{PP}, C_{top} and C_{AP} representing the carbon pool sizes (in t C ha^{-1}) of the passive pool, the top soil and the active pool, respectively. Size (C_{AP}) and pM (pM_{AP}) of the active pool are calculated numerically: In the two-pool model, every year a specific amount of carbon

input (I) with a specific pM value (pM_{litter}) enters the active pool as leaf and fine root litter. For the calculations presented here, litter input was assigned the pM value of atmospheric CO_2 of the respective year for deciduous leaf and fine root inputs (Equation 4). For needle input, a time lag of five years accounted for the time between carbon assimilation by the plant and needle fall (Equation 5).

$$pM_{litter}(t) = pM_{atmo}(t) \quad \text{for deciduous leaf and fine root input} \tag{4}$$

$$pM_{litter}(t) = pM_{atmo}(t-5) \quad \text{for needle input,} \tag{5}$$

where the subscript atmo refers to atmospheric CO_2.

Litter that has entered the active pool is subject to an exponential decay (Figure 2). Depending on the amount of carbon input (I) and the decay rate constant (k), the active pool reaches a defined pool size (C_{AP}) at a given time (Equation 6).

$$C_{AP}(t) = I(t) + C_{AP}(t-1) \times \exp(-k) \tag{6}$$

The amount of carbon input, its pM value and the decay rate constant also determine pM of the active pool carbon (pM_{AP}) at a given time (Equation 7).

$$pM_{AP}(t) \times C_{AP}(t) = pM_{litter}(t) \times I(t) + pM_{AP}(t-1) \times C_{AP}(t-1) \times \exp(-k) \tag{7}$$

Thus, pM_{AP} corresponds to the mixture of remaining litter from past years, each year's litter having a different pM value. Consequently, pM_{AP} changes continuously with time (Figure 3).

The decay rate constant (k) of the active pool (Equation 7) is adjusted, so that the numerically calculated mixture of passive pool and active pool carbon exactly matches the measured pM value of the top soil (pM_{top}) in the year of sampling (Equation 8).

$$pM_{top} = pM_{AP} \times \frac{C_{AP}}{C_{top}} + pM_{PP} \times \left(1 - \frac{C_{AP}}{C_{top}}\right) \tag{8}$$

The reciprocal of k is the turnover time (TT_{AP}) or mean residence time of the active pool (Equation 9). For steady state conditions, the turnover time equals the mean age of the active pool.

$$TT_{AP} = \frac{1}{k} \tag{9}$$

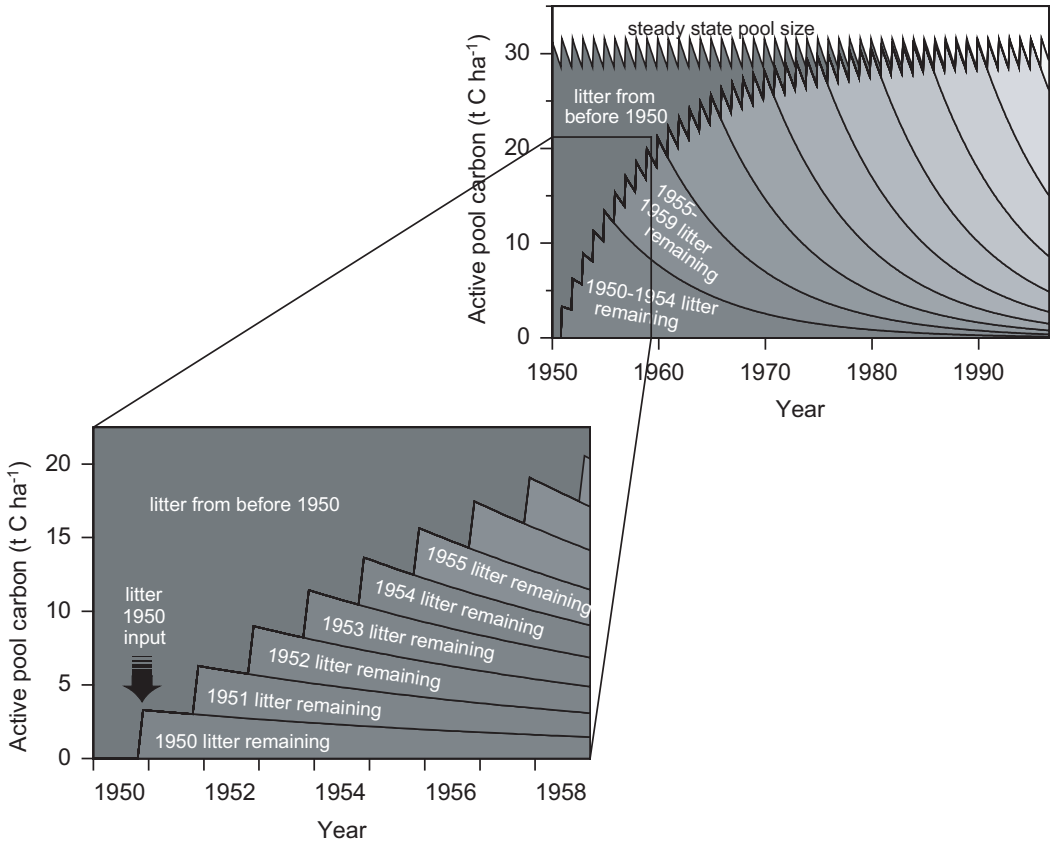

Figure 2. Development of active pool carbon from 1950 to 1996 according to the model, exemplary for the forest stand Collelongo. New litter is incorporated into the active pool every year. The litter decay follows an exponential function. The sum of all remaining litter forms the active pool.

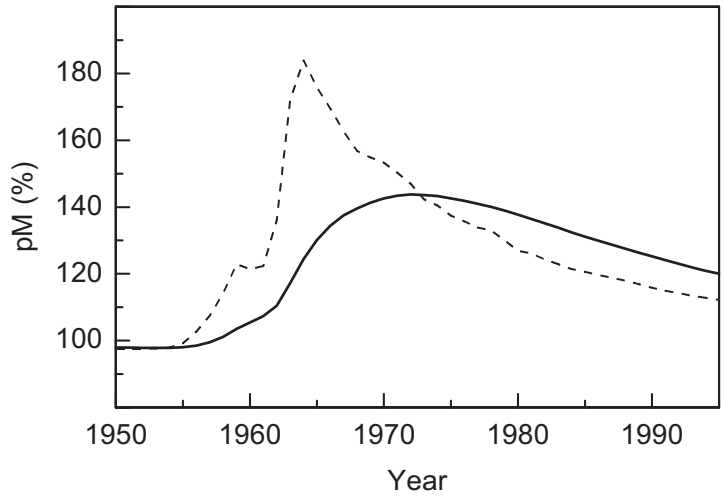

Figure 3. Modeled pM (percent Modern) value of active pool carbon under steady state conditions, exemplary for the forest stand Collelongo (solid line). The dashed line represents the pM value of atmospheric CO_2.

2.2.2 Site descriptions

Model calculations were performed for 25 European forest stands (Table 1). Nine of these stands were extensively investigated within the European research project CANIF (Persson et al. 2000). Another thirteen stands were investigated within FORCAST, the follow-up project of CANIF (both Fifth Framework Programme of the European Commission). Additionally, model calculations were performed for three forest stands that were experimentally manipulated in a girdling experiment (see chapter 3).

Table 1. Characteristics of investigated European forest stands.

Site name (country)	Main tree species	Stand age (yrs)	Latitude	Mean annual temp. (°C)	Annual precip. (mm)	Annual nitrogen deposition (kg N ha^{-1} yr^{-1})	Total soil organic carbon (t C ha^{-1})	Soil type (FAO)	Research project
Flakaliden (SE)	*Picea abies*	38[A]	64°07´N	1.0	567	2.7	67	Podzol	FORCAST
Sorø (DK)	*Fagus sylv.*	60[A]	55°29´N	8.1	510	11.8	196	Stagnic Phaeozem	FORCAST
Loobos (NL)	*Pinus sylv.*	80[A]	52°10´N	9.8	786	20.7	78	Dystric Cambisol	FORCAST
Hainich (DE)	*Fagus sylv.*	250[A]	51°05´N	7.0	750	26.2	83	Calcaric Cambisol	FORCAST
Hesse (FR)	*Fagus sylv.*	34[A]	48°40´N	9.2	885	14.9	61	Stagnic Luvisol	FORCAST
Leinefelde 30 (DE)	*Fagus sylv.*	30[A]	51°20´N	7.0	700	26.2	82	Rendzic Leptosol	FORCAST
Leinefelde 62 (DE)	*Fagus sylv.*	62[A]	51°20´N	7.0	700	26.2	64	Stagnic Luvisol	FORCAST
Leinefelde 111 (DE)	*Fagus sylv.*	111[A]	51°20´N	7.0	700	26.2	62	Haplic Luvisol	FORCAST
Leinefelde 153+15 (DE)	*Fagus sylv.*	153 & 15[A]	51°20´N	7.0	700	26.2	68	Stagnic Luvisol	FORCAST
Tharandt 5 (DE)	*Picea abies*	5[A]	50°58´N	7.5	824	22.0	262	Podzol	FORCAST
Tharandt 24 (DE)	*Picea abies*	24[A]	50°58´N	7.5	824	22.0	191	Podzol	FORCAST
Tharandt 42 (DE)	*Picea abies*	42[A]	50°58´N	7.5	824	22.0	154	Podzol	FORCAST
Tharandt 97 (DE)	*Picea abies*	97[A]	50°58´N	7.5	824	22.0	191	Podzol	FORCAST
Åheden*Picea* (SE)	*Picea abies*	180[B]	64°13´N	1.0	588	1.7	55	Regosol	CANIF
Skogaby (SE)	*Picea abies*	31[B]	56°33´N	7.6	1237	16.4	132	Haplic Podzol	CANIF
Nacetin (CZ)	*Picea abies*	58[B]	50°35´N	5.9	935	18.6	170	Spododystric Cambisol	CANIF
Waldstein (DE)	*Picea abies*	142[B]	50°12´N	5.5	890	20.1	202	Cambic Podzol	CANIF
Schacht (DE)	*Fagus sylv.*	120[B]	50°04´N	5.5	890	20.1	164	Dystric Cambisol	CANIF
Aubure*Picea* (FR)	*Picea abies*	92[B]	48°12´N	5.4	1192	14.7	54	Dystric Cambisol	CANIF
Aubure*Fagus* (FR)	*Fagus sylv.*	161[B]	48°12´N	5.4	1192	14.7	94	Haplic Podzol	CANIF
Collelongo (IT)	*Fagus sylv.*	108[B]	41°52´N	6.4	1109	10.8	228	Humic Alfisol	CANIF
Monte di Mezzo (IT)	*Picea abies*	37[B]	41°45´N	8.5	1032	n.a.	175	n.a.	CANIF
Åheden*Pinus* (SE)	*Pinus sylv.*	50[A]	64°13´N	1.0	588	1.7	n.a.	Podzol	Girdling
Wetzstein 35 (DE)	*Picea abies*	35[A]	50°27´N	5.6	880	20.9	n.a.	Podzol	Girdling
Wetzstein 114 (DE)	*Picea abies*	114[A]	50°27´N	5.6	880	20.9	177	Podzol	Girdling / FORCAST

[A] in year 2000,
[B] in year 1996
n.a. = not available

2.2.3 Model input

The two-pool model requires the amount and pM value of the top soil (C_{top}, pM_{top}) as well as the annual carbon input by above- and below-ground litter (I, pM_{litter}) as model input variables (Table 2). Most of these data were collected within the projects CANIF and FORCAST, some additional data (for the three girdled stands) were collected for this study.

To estimate amount and pM value of the top soil carbon, soil samples were taken by coring technique. Each core was separated into the L+F+H, 0-5 cm, 5-10 cm and 10-20 cm layers. After removing all roots, the soil samples were analyzed for C_{top} and pM_{top}. For further details on sampling and sample preparation, refer to Harrison et al. (2000). Data for the CANIF

stands were provided by Doug Harkness (NERC Radiocarbon Laboratory, East Kilbride, UK), data for the FORCAST stands by Phil Rowland (CEH Merlewood, Grange over Sands, UK). Samples from Åheden*Pinus* were provided by Anders Nordren (SLU, Umeå, Sweden), samples from the two Wetzstein stands were taken by myself. For details about sampling, sample preparations and analyses at Åheden*Pinus* and the two Wetzstein stands, refer to chapter 3.

Table 2. Model input.

Site name (country)	Year of sampling	Above-ground litter input (t C ha^{-1} yr^{-1})	Below-ground litter input (t C ha^{-1} yr^{-1})	Top soil depth (cm)	Top soil carbon (C_{top}) (t C ha^{-1})	Top soil percent Modern (pM_{top}) (%)
Flakaliden (SE)	2001	1.2	2.0	20	48.5	105.6
Sorø (DK)	2000	1.7	3.0	10	71.8	109.5
Loobos (NL)	2000	2.4	1.3	20	68.7	117.1
Hainich (DE)	2000	2.5	1.7	20	66.4	106.2
Hesse (FR)	2000	1.6	2.0	20	35.9	111.3
Leinefelde 30 (DE)	2000	2.0	2.8	20	60.7	110.5
Leinefelde 62 (DE)	2000	2.3	1.1	20	52.8	104.9
Leinefelde 111 (DE)	2000	2.4	1.2	20	47.5	105.0
Leinefelde 153+15 (DE)	2000	2.3	2.3	20	62.3	106.8
Tharandt 5 (DE)	2000	2.0	0.7	0[A]	99.8	110.0
Tharandt 24 (DE)	2000	2.0	1.8	20	127.7	105.9
Tharandt 42 (DE)	2000	2.0	1.8	20	76.1	109.7
Tharandt 97 (DE)	2000	2.0	1.4	20	112.2	105.5
Åheden*Picea* (SE)	1996	0.5	0.9	5	20.0	109.6
Skogaby (SE)	1996	1.3	2.8	10	52.7	105.0
Nacetin (CZ)	1996	1.8	0.6	5	51.0	108.2
Waldstein (DE)	1996	2.4	1.2	5	46.9	105.0
Schacht (DE)	1996	1.8	1.3	5	37.6	108.3
Aubure*Picea* (FR)	1996	1.1	0.4	20	46.0	111.5
Aubure*Fagus* (FR)	1996	1.4	0.8	10	40.9	109.5
Collelongo (IT)	1996	1.4	1.9	10	53.5	109.5
Monte di Mezzo (IT)	1996	1.4	1.5	20	76.8	109.4
Åheden*Pinus* (SE)	2001	0.5	0.7	20	35.5	108.5
Wetzstein 35 (DE)	2002	1.0	1.8	10	77.2	104.9
Wetzstein 114 (DE)	2002	1.8	1.4	5	63.7	107.5

[A] Bomb carbon only in the organic layer

Above-ground litter input was measured using litter traps at all thirteen FORCAST stands and the two Wetzstein stands. For the Hainich and the Leinefelde stands, data were provided by Martina Mund (Max Planck Institute for Biogeochemistry, Jena, Germany, *personal communication*), for all other FORCAST stands, data were provided by Francesca Cotrufo (University of Naples II, Italy). Litter fall at the Wetzstein stands was measured by myself (for details see chapter 3). For the CANIF stands, above-ground litter input via foliage was estimated by a full foliage biomass inventory, including tree felling, at seven of the ten CANIF stands (Scarascia-Mugnozza et al. 2000). Here, annual leaf litter input was estimated to be the same as annual leaf production. At Åheden*Picea* and Schacht, estimates of above-ground production were derived from volume and yield tables, after conversion of volumetric data into dry weights (Scarascia-Mugnozza et al. 2000). Note that above-ground litter fall data provided by Francesca Cotrufo and from the CANIF stands only include leaf or needle litter; for these stands, no litter fall data of twigs or buds could be obtained.

Below-ground litter input via fine roots was assessed by repeated soil core extractions at Collelongo, Monte di Mezzo, Aubure*Fagus* and Aubure*Picea*. For the remaining stands, fine root litter production was estimated assuming annual turnover of fine roots to equal fine root standing biomass. For a more detailed description of below-ground litter input estimates, refer to Scarascia-Mugnozza et al. (2000). Fine root data for the CANIF stands were taken from Scarascia-Mugnozza et al. (2000), data for the FORCAST stands were provided by Annelies Claus (Humboldt University Berlin, Germany, *personal communication*). At the Wetzstein stands, no below-ground litter input was measured; instead, values measured at two similar spruce stands were used (see chapter 3).

pM values of atmospheric CO_2 (pM_{atmo}) were taken from published data. I used data from Stuiver and Quay (1981) for the period from 1890 to 1955, data from Tans (1981) for 1955 to 1959 and data from Levin et al. (1985) for 1959 to 1984. For the years 1985 to 2002, pM values measured at the meteorological station Jungfraujoch (Swiss Alps) were provided by Ingeborg Levin (University of Heidelberg, Germany, *personal communication*). ^{14}C data of atmospheric CO_2 are listed in the Appendix.

2.2.4 Controlling factors

The relationships of modeled amounts and turnover times of active pool carbon with several environmental and stand variables were tested: latitude, mean annual temperature, annual

precipitation, annual nitrogen deposition, total soil organic carbon and stand age (Table 1). Linear regressions were calculated for the different combinations of variables.

2.2.5 Model sensitivity and soil carbon sequestration potential

Three tests were performed to assess the model´s sensitivity for calculating active pool turnover times and the potential of soils to sequester carbon. (1) Values of litter input were varied (from 70% to 130% of measured litter input), keeping all other variables constant. (2) The model was run for different values of pM_{PP} (from 85% to 100%), keeping litter input and all other variables constant. (3) The model´s reaction to a gradual increase of litter input by 50% and to a gradual increase of the active pool turnover time by 50% was tested, using 5% steps over 10 years. All three sensitivity tests were performed for the spruce stands Waldstein and Aubure*Picea*, and for the beech stand Collelongo. These three stands cover a wide range of calculated turnover times.

2.2.6 Experimental model validation

In addition to the turnover time, the model also calculates the pM value of the active pool carbon (pM_{AP}). Since the active pool - by definition - dominates SOC turnover, the CO_2 released by heterotrophic soil respiration should have a similar pM value as the active pool carbon. For the Hainich stand, this hypothesis was tested in order to validate the new model.

On April 21, 2001, mineral soil samples from 0-5 cm, 5-10 cm, 10-20 cm and 20-30 cm depth were collected from a fresh soil profile as well as additional samples from 10-20 cm soil depth at two replicate locations at the Hainich stand. After removing all roots, 155 to 635 g (depending on the carbon concentration) of the fresh soil material was incubated in exsiccators at 20 °C and 100% relative humidity. After 49 to 51 days, all exsiccators were flushed with CO_2-free air, and left for additional 10 to 15 days to accumulate new CO_2. The exsiccator head space air was then collected into pre-evacuated 2.3 l flasks. The CO_2 samples were isolated from other air constituents using a cryogenic vacuum line as described in Buchmann et al. (1997). The isolated CO_2 samples were quantitatively reduced to graphite and analyzed for pM. Measured pM values of respired CO_2 were compared to the pM values of the incubated SOC samples and to modeled pM values of the active pool at the Hainich stand. For details about CO_2 sampling, graphitization and analyses see chapter 3.

2.3 Results

2.3.1 Model results

Turnover times of the active pool (TT_{AP}) were calculated for 25 European forest stands. Turnover times varied by a factor of 4.1 among the different stands, ranging from 4.5 years at the German spruce stand Waldstein to 18.3 years at the German spruce stand Tharandt-5 (Table 3). The mean turnover time was 9.7 years. Turnover times varied relatively little among the respective stands of the two chronosequences (Tharandt and Leinefelde). Nevertheless, modeled values tended to decrease with stand age.

The modeled amounts of active carbon (C_{AP}) varied by a factor of 4.8 and ranged from 11.6 t C ha^{-1} at Åheden*Picea* to 55.7 t C ha^{-1} at Loobos (Table 3). The mean was 31.2 t C ha^{-1}.

Table 3. Model output.

Site name (country)	Year of sampling	Active pool Turnover time (yrs)	Active pool percent Modern (pM_{AP}) (%)	Active pool carbon (C_{AP}) (t C ha^{-1})	Active pool / top soil carbon ratio (C_{AP} / C_{top})
Flakaliden (SE)	2001	7.0	115.0	22.3	0.46
Sorø (DK)	2000	9.6	116.5	45.5	0.63
Loobos (NL)	2000	15.0	121.7	55.7	0.81
Hainich (DE)	2000	7.8	115.0	33.1	0.50
Hesse (FR)	2000	7.9	115.1	28.2	0.78
Leinefelde 30 (DE)	2000	8.8	115.9	42.9	0.71
Leinefelde 62 (DE)	2000	6.9	114.1	23.5	0.44
Leinefelde 111 (DE)	2000	6.1	113.4	22.3	0.47
Leinefelde 153+15 (DE)	2000	7.3	114.6	33.9	0.54
Tharandt 5 (DE)	2000	18.3	122.2	50.4	0.51
Tharandt 24 (DE)	2000	12.1	120.2	46.9	0.37
Tharandt 42 (DE)	2000	11.0	119.7	41.9	0.55
Tharandt 97 (DE)	2000	11.5	120.2	39.7	0.35
Åheden*Picea* (SE)	1996	7.5	118.5	11.6	0.58
Skogaby (SE)	1996	4.6	115.0	22.7	0.43
Nacetin (CZ)	1996	8.8	120.5	23.7	0.47
Waldstein (DE)	1996	4.5	115.3	19.8	0.42
Schacht (DE)	1996	6.0	116.3	21.5	0.57
Aubure*Picea* (FR)	1996	16.2	123.2	24.9	0.54
Aubure*Fagus* (FR)	1996	9.3	119.5	22.3	0.55
Collelongo (IT)	1996	8.2	118.5	30.5	0.57
Monte di Mezzo (IT)	1996	12.0	122.1	37.2	0.48
Åheden*Pinus* (SE)	2001	15.4	120.1	17.7	0.50
Wetzstein 35 (DE)	2002	10.5	117.0	29.0	0.38
Wetzstein 114 (DE)	2002	9.8	117.3	32.0	0.50

pM values of the active pool carbon (pM_{AP}) were much higher than those of atmospheric CO_2 at the time of sampling. Due to the decline of pM of atmospheric CO_2, calculated values of pM_{AP} were usually higher for the CANIF stands, which were sampled some years earlier than the other stands. Furthermore, pM values were usually high for the stands with low turnover and – due to the 5-year time lag before above-ground litter input – relatively high for conifer stands. Where pM_{AP} was high, the active pool contained a higher proportion of older carbon from the time when atmospheric CO_2 was more enriched in ^{14}C.

The ratio of active pool to top soil carbon (C_{AP}/C_{top}) varied considerably among stands, with values ranging from 0.35 at Tharandt-97 to 0.81 at Loobos.

2.3.2 Controlling factors

The relationships of modeled active pool turnover times (TT_{AP}) with potential factors controlling these turnover times, i.e., latitude, mean annual temperature, annual precipitation, annual nitrogen deposition, total soil organic carbon and stand age were tested (Table 1). N

However, no significant relationship was found for any of these variables. The best relationship was found for stand age, indicating a slight decrease in turnover time with increasing stand age ($P = 0.08$) (Figure 4).

The size of the active pool (C_{AP}) increased highly significantly with mean annual temperature ($P < 0.001$) (Figure 5). Like C_{AP}, also litter input increased highly significantly with mean annual temperature ($P = 0.001$) (Figure 6). Contrary, total soil organic carbon was not significantly related to mean annual temperature (not shown).

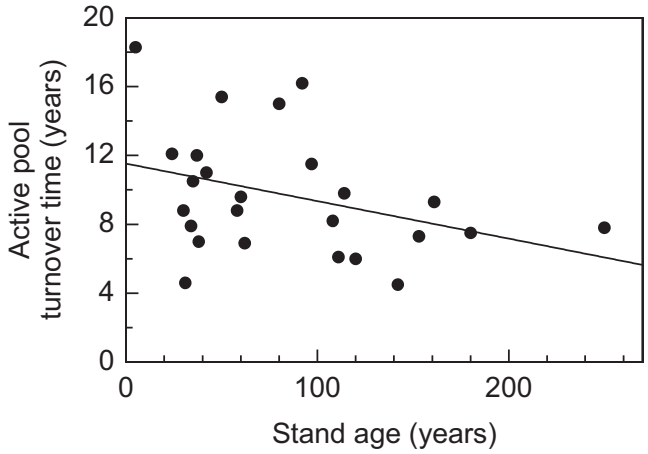

Figure 4. Modeled active pool carbon turnover time in relation to stand age. The solid line represents the linear regression (y = -0.022x + 11.5, R^2 = 0.129, *P* = 0.08).

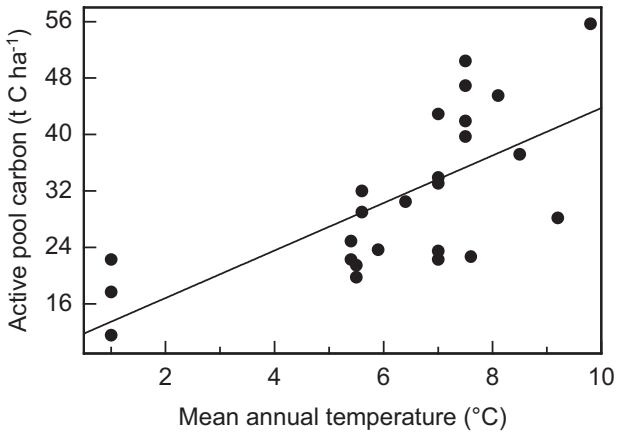

Figure 5. Modeled amount of active pool carbon (C_{AP}) in relation to mean annual temperature. The solid line represents the linear regression (y = 3.36x + 10.1, R^2 = 0.469, *P* < 0.001).

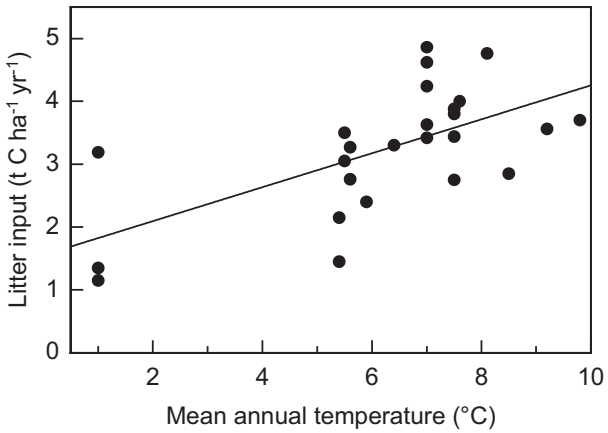

Figure 6. Measured above- plus below-ground litter input in relation to mean annual temperature. The solid line represents the linear regression (y = 0.27x + 1.6, R^2 = 0.394, *P* = 0.001).

2.3.3 Model sensitivity

For three forest stands, the model sensitivity against possible error sources for calculating the active pool turnover time was tested. First, the litter input was changed from 70% to 130% of measured litter input. For all stands, underestimating the litter input had a stronger effect on calculated turnover times than overestimating the litter input (Figure 7). For the two stands Waldstein and Collelongo, reducing litter input by 30% led to an increase of modeled turnover time by 31% (Waldstein) and 32% (Collelongo). However, for Aubure*Picea*, the same change in litter input resulted in an increase of turnover time by 54%. Increasing the litter input rate by 30% leads to comparatively small decreases in turnover times of 18% (Collelongo), 19% (Waldstein) and 23% (Aubure*Picea*).

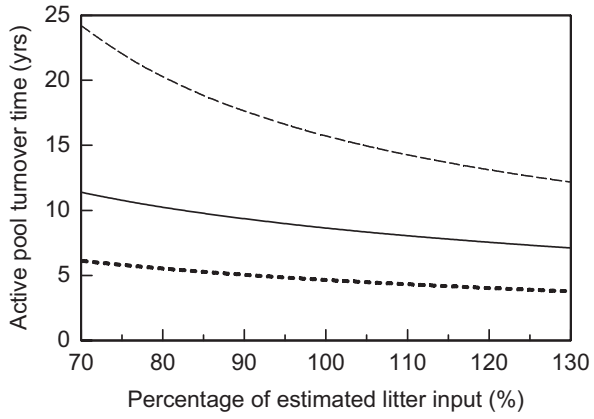

Figure 7. Modeled active pool turnover time in relation to litter input. Litter input was varied from 70% to 130% of measured litter input (see Table 2). Exemplary calculations for AuburePicea (dashed line), Collelongo (solid line) and Waldstein (dotted line).

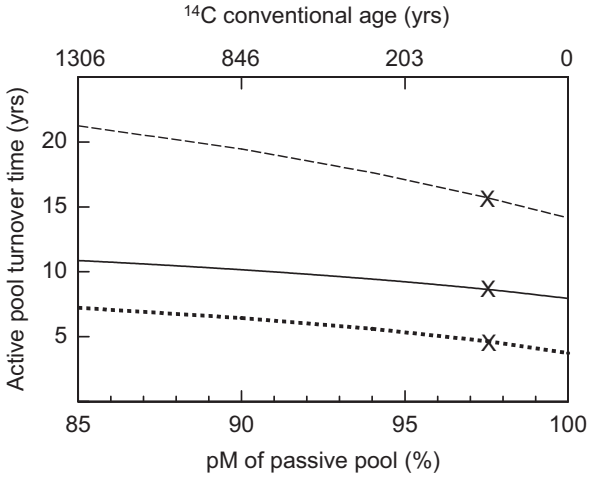

Figure 8. Modeled active pool turnover times in relation to pM and ^{14}C conventional age of the passive pool. For values >500 years, the ^{14}C conventional age corresponds ± to the time when atmospheric CO_2 had the pM value shown on the bottom x axis. pM_{PP} was varied from 85% to 100%. Exemplary calculations for AuburePicea (dashed line), Collelongo (solid line) and Waldstein (dotted line). The crosses indicate the pM value used in the model (pM_{PP} = 97.5%).

Secondly, the sensitivity of modeled turnover times against the assumption that the passive pool has a pM value of 97.5% was tested (Figure 8). If the passive pool contained much carbon older than 500 years, this carbon would decrease pM_{PP} to values below 97.5%. For pM_{PP} = 90%, which corresponds to a ^{14}C conventional age of 846 years, calculated turnover times would increase by 17% (Collelongo), 24% (Aubure*Picea*) and 38% (Waldstein). A pM_{PP} value of 85% (^{14}C conventional age = 1306 years) would increase turnover times by

26% (Collelongo), 35% (Aubure*Picea*) and 55% (Waldstein), respectively. The Waldstein stand is more sensitive to a change in pM_{PP} than the other two stands because of its lower active pool to top soil carbon ratio ($C_{AP}/C_{top,}$ Table 3).

2.3.4 Experimental model validation

To validate the model, heterotrophically respired CO_2 was collected and its pM value was compared with the modeled pM value of the active pool carbon (pM_{AP}) at the Hainich stand.

Large differences were found between the pM values of the incubated mineral soil samples (carbonate free) from the Hainich stand and the pM values of CO_2 respired from the same soil samples (Table 4). pM values of respired CO_2 was 3.2% to 12.8% higher (ΔpM) than pM values of the corresponding SOC, with a mean difference of 9.6%. This clearly shows that the assumption made in most ^{14}C turnover models, i.e., that the carbon lost from a soil fraction by respiration has the same ^{14}C content as the soil material it originates from, is incorrect.

Table 4. Laboratory incubations of soil from the Hainich stand.

Soil depth (cm)	Soil profile #	pM of soil organic carbon (%)	pM of respired CO_2 (%)	Mean CO_2 respiration rate during first 10 days of incubation (mg C g C^{-1} day^{-1})	Soil organic carbon content in the field (t C ha^{-1})
0-5	1	107.6	119.1	1.20	25.3
5-10	1	109.5	117.2	0.86	18.6
10-20	1	104.6	107.8	0.37	25.4
10-20	2	95.9	106.0	0.28	25.4
10-20	3	98.0	110.8	0.30	25.4
20-30	1	92.9	104.9	0.21	12.3

The weighted mean pM value of respired CO_2, accounting for respiration rates and carbon contents of the different soil depths, was 116.4%. This value agrees considerably well with pM_{AP} calculated for the Hainich stand (pM_{AP} = 115.0%).

2.3.5 Soil carbon sequestration potential

Using the new model, the potential of soils to sequester carbon was tested by simulating gradually increasing litter inputs as well as increasing turnover times.

Increasing the litter input by 50% caused an increase in the active pool size by also 50% after 30 to 40 years (Figure 9). Annual carbon sequestration showed maximum values of 0.8 (Waldstein), 1.0 (Collelongo) and 0.6 t C ha^{-1} yr^{-1} (Aubure*Picea*), but decreased sharply once litter input remained at a high but constant level. Increasing the turnover time by 50% caused

an increase in the active pool size by 45% (Waldstein), 47% (Collelongo) and 48% (Aubure*Picea*) after 40 to 50 years (Figure 10). Annual carbon sequestration showed maximum values of 0.6 (Waldstein), 0.7 (Collelongo) and 0.4 t C ha^{-1} yr^{-1} (Aubure*Picea*). Thus, the response of the active carbon pool was quite similar to that after a comparable increase of litter input.

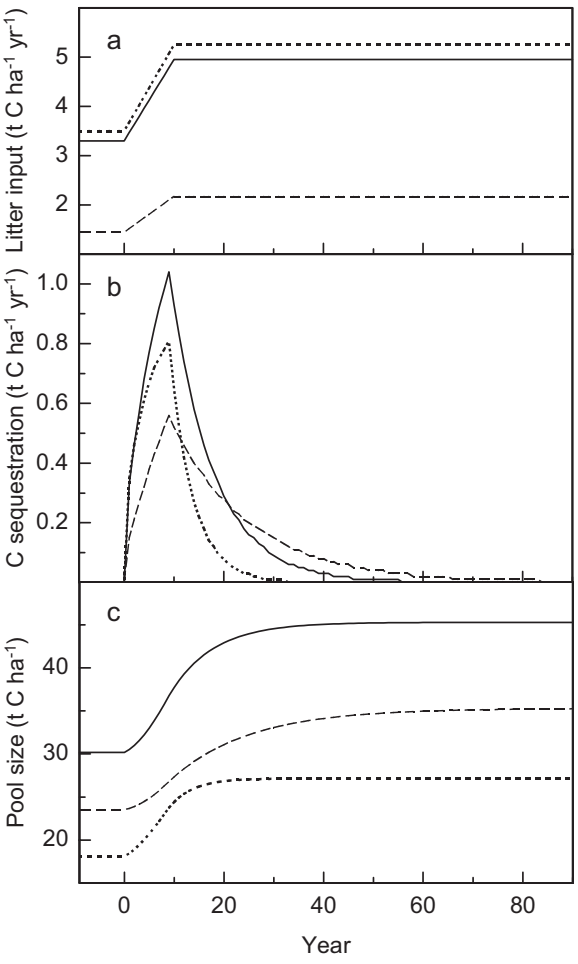

Figure 9. Modeled changes in (b) active pool carbon sequestration and (c) active pool size following a 50% increase in (a) litter input. Exemplary calculations for Aubure*Picea* (dashed line), Collelongo (solid line) and Waldstein (dotted line).

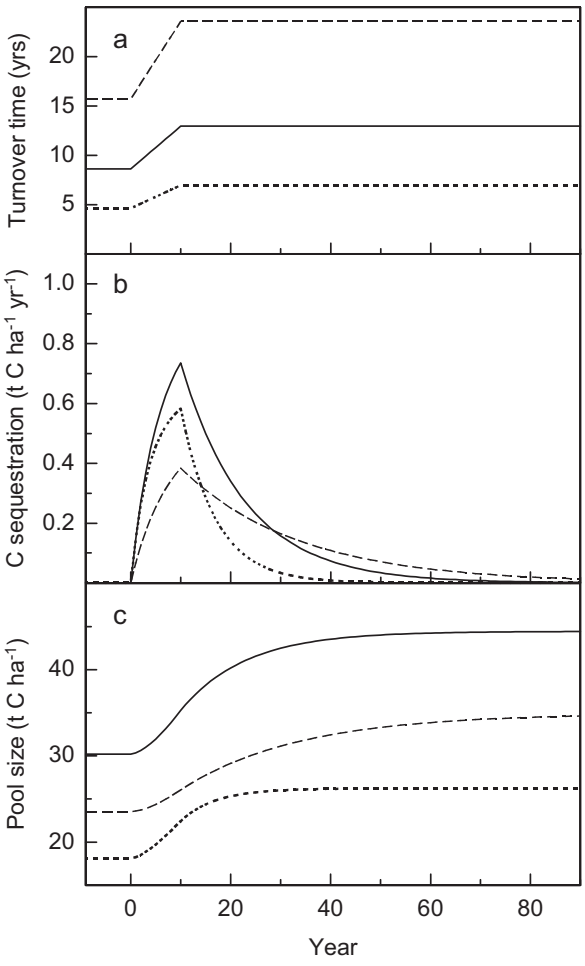

Figure 10. Modeled changes in (b) active pool carbon sequestration and (c) active pool size following a 50% increase in (a) active pool turnover time. Exemplary calculations for Aubure*Picea* (dashed line), Collelongo (solid line) and Waldstein (dotted line).

2.4 Discussion

I developed and tested a new model for calculating the turnover time of active soil organic carbon using bomb carbon as a tracer.

The new model was designed to overcome the two major deficiencies of older ^{14}C models, where (1) the current atmospheric ^{14}C content is used for carbon input into all soil depths and soil fractions and (2) the ^{14}C content of CO_2 respired from SOC or SOC fractions has the same ^{14}C content as the SOC (fraction) itself. Contrary, in the new model, litter originating from living biomass is incorporated directly into an active carbon pool that spreads over the entire profile of the top soil. The advantage of this new approach is that pM of litter input from living biomass is relatively easy to measure or estimate. Furthermore, in the new model, SOC of the top soil consists of two pools (active and passive), and carbon lost from the top soil carbon has the ^{14}C content of the active pool carbon, not that of total SOC. Therefore, the model accounts for the presence of recalcitrant carbon that may not contribute to SOC respiration. This new approach is confirmed by the results of the soil incubation experiments, which clearly showed that CO_2 respired from SOC has a much higher pM value than the SOC itself (Table 4).

The model was validated by comparing the calculated pM values of the active pool to pM values of CO_2 respired from root free soil during incubation. Good agreement was found, which confirms the new model approach.

The model sensitivity against possible errors in estimating (1) the amount of litter input (I), and (2) the pM value of the passive pool (pM_{PP}) was tested. (1) Litter input was shown to be an important input variable for the model. Errors in estimating the amount of litter input can alter modeled turnover times, especially if the litter input is underestimated (Figure 7). This is particularly critical since the below-ground litter input by roots is difficult to measure. ^{14}C measurements of fine roots suggested lower fine root turnover than other methods like root-viewing cameras (Gaudinski et al. 2001). Tierney and Fahey (2002) have reconciled the discrepancies in these different measurement techniques of root turnover. They propose that a skewed distribution of root age leads to an overestimation of root turnover by visual techniques and an underestimation by the ^{14}C technique. Further progress in estimating below-ground litter input will also increase the precision of the presented model.

(2) In the new model, it is assumed that pM_{PP} = 97.5%, which corresponds to the mean pM value of atmospheric CO_2 from 1500 to 1950 (Figure 1). But in fact, the passive pool could

have a pM value lower than 97.5%, if the top soil contained much carbon older than 500 years. For example, the calculated turnover time of the active pool would be 17 to 38% too high, if pM_{PP} had a real value of 90% instead of 97.5% (Figure 8). However, such a low pM value seems unlikely as this would correspond to a mean (!) ^{14}C conventional age of 846 years. Archived soil samples suggest that SOC had a mean pM value close to 97.5% in depths to 20 cm before bomb carbon was incorporated (O'Brien and Stout 1978, Torn et al. 2002, Wang et al. 1999). Trumbore and Zheng (1996) applied physical and chemical fractionations to a variety of soil samples. Their data suggest that soil samples with a mean pM value higher than 97.5% contained only little carbon with pM < 97.5%. Accordingly, they also found little carbon with pM > 97.5% in soil samples with a mean pM value < 97.5%. It should be possible to further increase the precision of the new model by fractionating soil samples before ^{14}C analysis and only account for those carbon fractions that contain bomb carbon (i.e., fractions with pM > 97.5%).

Using the new model is easy and the number of necessary ^{14}C measurements is comparatively low. Once it is known, at what depth the top soil ends, i.e., where active carbon is present (pM_{top} > 97.5%), only one soil sample is needed for C and ^{14}C content analyses. No soil fractionation is necessary (although desirable). However, annual litter input must be available, since it is a critical model input variable (Figure 7). Another prerequisite is that no major of erosion of in-situ soil carbon or accumulation of ex-situ carbon occurred since 1950.

The model was applied to calculate active pool turnover times for 25 European forest stands. Large differences were found among the stands with turnover times varying by a factor of 4.1. The best linear regression of turnover times with different environmental and stand variables was found for stand age, indicating decreasing turnover times with stand age (Figure 4). Similarly, turnover times of the chronosequence stands tended to decrease with age (Table 3). At young stands, tree harvest occurred only a few years ago. Harvest can involve a high one-time input of ^{14}C rich woody debris into SOC. This input may be the main reason for higher modeled turnover times. Ideally, litter input and its ^{14}C content should be measured or assessed individually for every single year, especially for recent years and years of thinning or harvest. Unfortunately, this was not feasible within the scope of this study.

In addition to turnover times, the model also calculates the amount of the active pool carbon (C_{AP}). C_{AP} increased highly significantly with mean annual temperature (3.4 t C ha^{-1} $°C^{-1}$). This suggests that climatic changes involving increasing temperatures may increase SOC

stocks and cause net carbon sequestration. Potential mechanisms will be discussed in more detail in chapter 5.

Soils are believed to potentially sequester large amounts of carbon under changing climatic conditions. E.g., Schulze et al. (2000) suggest current mean soil carbon sequestration rates of 1.4 t C ha^{-1} yr^{-1} for 11 investigated European forest stands. Based on my results, I consider the potential of soils to sequester carbon much smaller. High carbon sequestration cannot occur in the recalcitrant carbon pool, which has accumulated over thousands of years and turns over very slowly. Annual carbon inputs into this recalcitrant pool must have been very small, or otherwise, the recalcitrant carbon pools would be much larger than they are today. E.g., assuming a recalcitrant carbon pool size of 100 t C ha^{-1} today, a build-up time of 10,000 years since the last glacial and a turnover time of 1,000 years, the annual carbon input into the recalcitrant pool would have to be 0.1 t C ha^{-1} yr^{-1} (for a mean European forest soil). However, SOC with such small annual carbon inputs cannot be accountable for high carbon sequestration, as the SOC pool cannot sequester more carbon than it receives by carbon inputs. Only the active carbon pool, which receives high annual carbon inputs by leaf and root litter, can potentially sequester large amounts of carbon. Because of its fast turnover, the active carbon pool reaches a steady state relatively fast, i.e., within decades (Figure 2). Carbon sequestration can only be achieved if either (1) the input of litter carbon increases or (2) the carbon turnover time increases. However, model calculations for three forest stands showed that even an increase of litter input or turnover time by unexpected 50% under changing climatic conditions does not result in high carbon sequestration over long time periods (Figures 9 and 10). In contrast, carbon sequestration diminished quickly, once litter input or turnover time stopped increasing. Therefore, if soils sequester carbon, it is the result of a transitory disequilibrium. Soils cannot be accountable for long-term and persistent high ecosystem carbon sequestration under future climatic conditions.

3 Separating heterotrophic and autotrophic soil respiration

3.1 Introduction

One of the largest uncertainties in our understanding of the terrestrial carbon cycle is the partitioning between heterotrophic and autotrophic soil respiration. A variety of methods has been developed and was reviewed by Hanson et al. (2000). Techniques include component integration [extrapolation of individual SOC and root CO_2 production measurements (Edwards and Sollins 1973, Ewel et al. 1987, Gansert 1994, Thierron and Laudelout 1996)], root exclusion [e.g., trenching (Boone et al. 1998, Bowden et al. 1993, Epron et al. 1999, Janssens et al. 2003b)], and isotopic methods [natural and pulse labeling (Högberg and Ekblad 1996, Kuzyakov and Cheng 2001, Lin et al. 1999, Swinnen et al. 1994)].

Probably the most robust method to experimentally separate autotrophic and heterotrophic respiration is tree girdling. Girdling involves stripping the stem phloem to the depth of the xylem, thus terminating the supply of photosynthates to the roots and their mycorrhizal fungi. As a result, tree-girdling reduces autotrophic respiration to a minimum, leaving heterotrophic respiration as the dominant CO_2 source. Högberg et al. (2001) measured flux rates of soil respired CO_2 in girdled and control plots in order to calculate contributions of heterotrophic and autotrophic respiration to total soil respiration. However, tree girdling is labor-intensive and destructive. For obvious reasons, the method can only be applied to a small selection of forest stands, especially in regions where the forested area is small or protected.

Another equally promising tool that is non-destructive and that can also be applied to non-forest soils is the use of the ^{14}C content of CO_2. Heterotrophically respired CO_2 has been shown to be enriched in ^{14}C compared to current atmospheric CO_2 (Certini et al. 2003, Gaudinski et al. 2000, Koarashi et al. 2002, Tegen and Dörr 1996, Wang et al. 2000). The ^{14}C content of autotrophically respired CO_2, in turn, corresponds to that of atmospheric CO_2 (Dörr and Münnich 1986, Wang et al. 2000). Therefore, ^{14}C of soil respired CO_2 bears potential for separating heterotrophic and autotrophic soil respiration.

Different approaches how to use ^{14}C for estimating hetero- vs. autotrophic soil respiration can be found. Wang et al. (2000) assumed that autotrophic respiration is relatively low in autumn due to physiological changes during dormancy. Therefore, they argued, heterotrophic

respiration dominates, and thus the ^{14}C content of heterotrophically respired CO_2 should correspond to the ^{14}C content of total soil respired CO_2 in autumn. This assumption is rather questionable and has not been verified. Furthermore, it seems invalid in areas, where plant activity is continuously high. Thus, other approaches to determine the ^{14}C content of heterotrophically respired CO_2 are needed.

In various models, ^{14}C has been used to calculate turnover times of SOC. Although all of these models can potentially be used to calculate the ^{14}C content of heterotrophically respired CO_2, this has rarely been done so far. E.g., Gaudinski et al. (2000) calculated the ^{14}C content of CO_2 respired from "Reservoir-C", which did not include soil organic carbon cycling on time-scales of less than one year.

The most frequently used ^{14}C turnover model is the box model (e.g., Gaudinski et al. 2000, Harkness et al. 1986, Hsieh 1993, O'Brien and Stout 1978, Trumbore et al. 1989, Trumbore et al. 1996, Wang et al. 1996). The box model assumes an annual input and output of carbon (of the same magnitude) into and out of different SOC compartments ("boxes"). These boxes can be soil horizons, depths, physical or chemical fractions. The ^{14}C content of the input carbon into the plant box equals the ^{14}C content of atmospheric CO_2, but in the model one has to account for the residence time of carbon in the plant before it can be incorporated into the soil. The ^{14}C content of the output carbon equals that of any given box in the respective year. The turnover is adjusted for each box, so that the calculated ^{14}C content of the box matches that measured in the year of sampling. Accounting for turnover rates and box sizes, the output carbon flux from each box can be calculated. This output carbon flux is a purely respiratory flux. By weighting the ^{14}C content of CO_2 respired from each of the different soil boxes by their output fluxes, the mean ^{14}C content of heterotrophically respired CO_2 can be calculated.

The cascade model was developed based on the box model (Harrison et al. 2000). But other than the box model, the cascade model assumes a downward transfer of SOC from one box to the next ("cascade"). Therefore, the ^{14}C content of the input carbon equals that of the overlying box. Turnover rates and output carbon fluxes are calculated as for the box model. The output carbon flux from a soil box is divided into a respiratory flux and a transfer flux to the underlying box, with the respiratory carbon flux being calculated as the difference of carbon flux through this box and its underlying box.

The two-pool model was presented in chapter 2. This model calculates the ^{14}C content of the active carbon pool. Since the active pool, by definition, dominates heterotrophic soil respiration, heterotrophically respired CO_2 has the same ^{14}C content as the active pool.

In this study, the potential of ^{14}C for partitioning heterotrophic and autotrophic soil respiration was evaluated for three girdled forest stands in Sweden and Germany. My objectives were (1) to measure and assess the differences in the ^{14}C contents of hetero- and autotrophically respired CO_2, (2) to quantify the contributions of heterotrophic respiration to total soil respiration using two different experimental approaches and (3) to compare measured and modeled ^{14}C contents of heterotrophically respired CO_2 and the thereby calculated contributions of heterotrophic respiration to total soil respiration.

3.2 Methods

3.2.1 Sites

For this study, 3 of the 25 forest stands of chapter 2 were investigated in more detail. Åheden*Pinus* is a 50-year-old Scots pine (*Pinus sylvestris* L.) forest in Northern Sweden (64°13´N, 19°46´E, 175 m asl). The soil is a weakly podzolized sandy silt. Wetzstein is a Norway spruce (*Picea abies* (L.) Karst.) forest area in Southern Thuringia, Germany (50´27°N, 11´27°E, 750 m asl). Soils are podzolized sandy loam. The bedrock is quarzite. At Wetzstein, a 35-year-old (Wetzstein 35) and a 114-year-old (Wetzstein 114) stand were investigated. The old stand has understory vegetation of grasses and bilberry (*Vaccinium myrtillus* L.), while the young stand has no understory.

3.2.2 Girdling

Trees at Åheden*Pinus* were girdled in June (early girdled) or August (late girdled) 2000 (Högberg et al. 2001). Six girdled and three control plots of 900 m^2 each were established. Trees at the two Wetzstein stands were girdled in April 2001, each stand consisting of three girdled and three control plots. In the young stand, the plot size was 400 m^2, in the old stand 900 m^2.

3.2.3 CO_2 sampling and flux measurements

At Åheden*Pinus*, CO_2 flux measurements and sampling were performed at four girdled (three early girdled and one late girdled) and three control plots on August 13, 2001, i.e., roughly 12 months after the late girdling and 14 months after the early girdling in 2000. All twelve plots

at the Wetzstein (six in Wetzstein 35 and Wetzstein 114, respectively) were measured and sampled on July 24 and July 25, 2002, respectively.

Soil respired CO_2 was sampled using stainless steel chambers, which form a static headspace above the soil surface (Figure 11). Stainless steel rings (300 mm in diameter, 100 mm height) were placed on the soil floor several months before sampling. For sampling, a stainless steel lid connected to a stainless steel capillary (ID 1.0 mm) was placed on top of the ring to form a closed chamber. A pre-evacuated flask (2.3 l) was connected to the capillary, with a $Mg(ClO_4)_2$ tube placed between flask and capillary to free the sampled air from H_2O. Lids were left on the chamber rings for 30 minutes to let soil respired CO_2 accumulate in the chamber. The long sampling time was necessary to collect sufficient CO_2 for the ^{14}C analyses. Afterwards, the flask valve was opened to draw the chamber air into the flask. One (Åheden*Pinus*) or three (Wetzstein) samples were collected per plot. For each of the Wetzstein stands, one additional free air sample was collected from approximately 5 cm above the forest floor, using a 2.3 l flask connected to a $Mg(ClO_4)_2$ tube and a stainless steel capillary (ID 1.0 mm) with an open end.

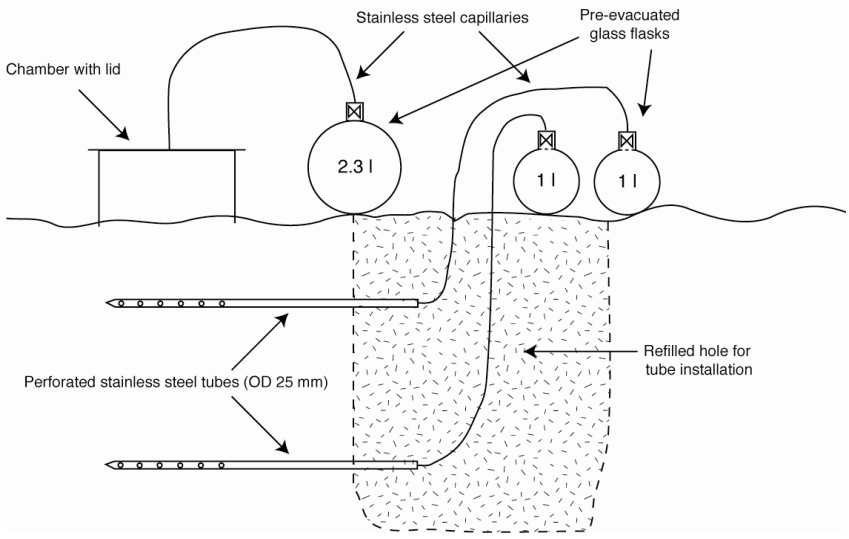

Figure 11. Sampling techniques for soil respired CO_2 (this chapter) and soil CO_2 (for details see next chapter).

Flux rates of soil respired CO_2 were measured approximately 30 minutes prior to CO_2 sampling, using a Licor 6400-9 infra red gas analyzer (Licor, Nebraska, USA). Two plastic rings (100 mm diameter, 80 mm height) that were placed inside the stainless steel chamber rings were used for measurements (three cycles per plastic ring). These plastic rings were inserted into the soil several months before sampling.

3.2.4 Isotopic units

^{13}C content is given as

$$\delta^{13}C = \left(\frac{R_{sample}}{R_{standard}} - 1 \right) \times 1000\ ‰, \quad (10)$$

where R_{sample} is the molar $^{13}C/^{12}C$ ratio of the sample and $R_{standard}$ is the molar $^{13}C/^{12}C$ ratio of the international VPDB standard [based on the CG99 scale (CSIRO-AR)]. The ^{14}C content is given in pM (Equation 2).

3.2.5 Analyses

Mixing ratios of CO_2 ($[CO_2]$) and N_2O (needed for a correction of $\delta^{13}C$) were measured using a gas chromatograph equipped with a flame ionization detector and an electron capture detector (Agilent 6890, Palo Alto, CA, USA) (Jordan and Brand 2001).

$\delta^{13}C$ values of atmospheric CO_2 were measured using an isotope ratio mass spectrometer (Finnigan MAT 252, Bremen, Germany) coupled to an automated cryogenic CO_2 extraction line (Werner and Brand 2001). For air samples with $[CO_2] > 400$ ppm (i.e., all chamber samples), the sampling time at the extraction line was reduced proportionally in order to obtain similar signal strengths for sample and reference gas ($[CO_2] \sim 360$ ppm).

After $[CO_2]$ and $\delta^{13}C$ measurements were completed, the sample CO_2 was isolated, graphitized and analyzed for pM as described in chapter 2.

3.2.6 Corrections

Measured isotopic values had to be corrected in order to account for atmospheric CO_2 that was already in the chamber when the lid was placed for sampling, using a simple isotope mixing-model:

$$\delta^{13}C_{respired} = \frac{\delta^{13}C_{chamber} \times [CO_2]_{chamber} - \delta^{13}C_{free\ air} \times [CO_2]_{free\ air}}{[CO_2]_{chamber} - [CO_2]_{free\ air}} \quad (11)$$

The same correction was applied to A, which is the ^{14}C activity of the sample. pM of soil respired CO_2 was obtained by combining the corrected values of A and $\delta^{13}C$ (Equation 2).

3.2.7 Modeling pM of heterotrophically respired CO_2

Three different models were applied to calculate pM of heterotrophically respired CO_2 in the three stands: box model, cascade model and two-pool model.

The same residence times of carbon in the plant and the same pM values of atmospheric CO_2 were used as described in chapter 2.

For both box and cascade model, carbon output fluxes of CO_2 respired from each box were calculated as

$$F_{out\,i} = \frac{C_i}{TT_i}, \tag{12}$$

where F_{out} is the output flux (amount carbon area^{-1} time^{-1}), C is the box pool size (amount carbon area^{-1}) and TT is the calculated turnover time.

For the cascade model, respiratory carbon fluxes were calculated as

$$F_i = F_{out\,i} - F_{out\,i+1}, \tag{13}$$

where the subscript i indicates the different soil boxes, counting from top to bottom. Negative values of F_i were changed to zero. For the bottom soil box in the cascade model and for all boxes in the box model, respiratory fluxes equal output fluxes:

$$F_i = F_{out\,i} \tag{14}$$

The mean pM value of heterotrophically respired CO_2 is calculated as

$$pM_{mean} = \frac{\sum_{1}^{n}(pM_i \times F_i)}{\sum_{1}^{n} F_i}, \tag{15}$$

where i indicates the different SOC boxes. For the two-pool model, the pM value of heterotrophically respired CO_2 equals that of the active pool.

3.2.8 Model input

Model input values were carbon amounts and pM values of the different soil layers and the annual carbon input by above- and below-ground litter (Table 5). Eight soil cores were randomly sampled at each stand (only control plots) using corers of 42 or 48 mm diameter.

Åheden*Pinus* was sampled on September 10, 2002, whereas the two Wetzstein stands were sampled on October 29 and 30, 2002. The samples were divided into four soil layers: L+F+H (organic layer), 0-5 cm, 5-10 cm and 10-20 cm. Sample 1 to 4 and 5 to 8 were mixed for each soil layer, leaving two composite samples per layer and stand. Roots were extracted from all samples by hand. After drying (70 °C, 72 h), the soil samples were weighed, and subsamples were analyzed for carbon concentrations to calculate carbon pool sizes for all soil boxes (mass carbon area^{-1}). A second subsample was analyzed for pM.

Table 5. Input values used for modeling pM values of heterotrophically respired CO_2.

	Åheden*Pinus*		Wetzstein 114		Wetzstein 35	
	pM (%)	Pool (t C ha^{-1})	pM (%)	Pool (t C ha^{-1})	pM (%)	Pool (t C ha^{-1})
L+F+H	117.7	11.0	112.1	40.2	109.7	37.8
0 - 5 cm	107.6	10.8	99.5	23.5	100.8	27.0
5 - 10 cm	102.4	6.5	94.9	20.5	99.0	12.4
10 - 20 cm	101.3	7.2	86.2	33.3	96.3	19.8
	Litter input (t C ha^{-1} yr^{-1})					
Above-ground	0.45[A]		1.80		0.97	
Below-ground	0.70		1.41[B]		1.77[B]	

[A] measured at the adjacent spruce stand Åheden*Picea*,
[B] measured at a 97-year-old (for Wetzstein 114) and a 42-year-old (for Wetzstein 35) stand of a comparable spruce site in Tharandt, Germany

Above-ground litter input was measured at the Wetzstein control plots from May 27, 2002 to June 11, 2003 using 18 litter traps (0.5 m^2 each) per stand. For Åheden*Pinus*, above-ground litter input data of the adjacent conifer site Åheden*Picea* was used (Scarascia-Mugnozza et al. 2000). For the Wetzstein stands, data of fine root standing biomass were taken from two stands (42- and 97-year-old) at the similar Norway spruce site Tharandt (Table 1) (Annelies Claus, Humboldt-University Berlin, *personal communication*). For Åheden*Pinus*, fine root standing biomass data were taken from Plamboeck et al. (1999). The annual below-ground litter input was set to equal the fine root standing biomass.

3.2.9 Fractions of soil respiration components

The contributions of heterotrophic respiration to total soil respiration were calculated using two approaches, with flux rates and with pM values of respired CO_2. Based on flux rates, the fraction of heterotrophic soil respiration (h_{flux}) was calculated as:

$$h_{flux} = \frac{F_G}{F_C} \times 100\ \%, \qquad (16)$$

where F_G is the flux rate (amount carbon area^{-1} time^{-1}) of soil respired CO_2 in the girdled plots and F_C is the flux rate in the control plots.

Based on ^{14}C, the fraction of heterotrophic soil respiration (h_{flux}) was calculated as:

$$h_{pM} = \frac{pM_C - pM_{auto}}{pM_{hetero} - pM_{auto}} \times 100\,\%, \tag{17}$$

where the subscript C denotes CO_2 respired in the control plots and the subscript hetero denotes heterotrophically respired CO_2, either measured in the girdled plots or calculated by one of the three models. The subscript auto denotes autotrophically respired CO_2. Since plant roots respire mainly recently assimilated carbon (Ekblad and Högberg 2001, Högberg et al. 2001, Horwath et al. 1994), pM_{auto} can be assumed to equal pM of current atmospheric CO_2 (Dörr and Münnich 1986, Wang et al. 2000):

$$pM_{auto} = pM_{atmo} \tag{18}$$

For Åheden*Pinus*, pM_{atmo} was taken from measurements at the atmospheric observation station Jungfraujoch, Swiss Alps (Ingeborg Levin, University of Heidelberg, *personal communication*). For the Wetzstein stands, pM_{atmo} equals pM of the free air samples taken on the day of sampling.

Standard errors of h_{flux} and h_{pM} were calculated as

$$SE_{h_{flux}} = \sqrt{\left(\frac{SE_{F_G}}{F_G}\right)^2 + \left(\frac{SE_{F_C}}{F_C}\right)^2} \times h_{flux} \tag{19}$$

and

$$SE_{h_{pM}} = \sqrt{\left(\frac{SE_{pM_G}}{pM_G - pM_{auto}}\right)^2 + \left(\frac{SE_{pM_C}}{pM_C - pM_{auto}}\right)^2} \times h_{pM}, \tag{20}$$

where SE_F and SE_{pM} are the standard errors of measured flux rates or pM values in girdled and control plots, respectively.

The autotrophic fraction of soil respiration (a) was calculated as:

$$a = 100\,\% - h \tag{21}$$

For the Wetzstein stands, two-way ANOVAs were performed to compare pM values and flux rates of soil respired CO_2. *Stand age* and *treatment* (girdled vs. control plots) were tested as independent and interactive sources of variance. When the interaction term was not

significant, a Tukey´s post-hoc test was performed to separate between the means. For the Åheden*Pinus* stand, one-way ANOVAs were performed to compare pM values and flux rates. Here, *treatment* was the single source of variance.

3.3 Results

Flux rates of soil respired CO_2 were measured in both girdled and control plots. Flux rates were always higher in the control plots compared to the girdled plots (Figure 12). While soil respiration in the control plots varied strongly from stand to stand, flux rates in the girdled plots were similar. Even the Åheden*Pinus* stand, measured one year earlier, showed similar flux rates in the girdled plots as the Wetzstein stands. While *treatment* (i.e., girdling or control) was a significant ($P < 0.05$) source of variation for the Wetzstein stands, it was not significant for the Åheden*Pinus* stand. *Stand age* (i.e., Wetzstein 35 or 114) was not significant for the Wetzstein stands (Table 6).

At all three stands, pM of soil respired CO_2 was higher in the girdled plots (Figure 13). Girdling leaves heterotrophic respiration as the major source of soil respired CO_2. Therefore, the results agree with several studies, which have shown that heterotrophically respired CO_2 is enriched in ^{14}C compared to autotrophically respired CO_2 (Certini et al. 2003, Koarashi et al. 2002, Tegen and Dörr 1996, Wang et al. 2000). For both girdled and control plots, pM decreased in the order Åheden*Pinus* > Wetzstein 114 > Wetzstein 35, ranging from 116.9% in girdled plots at Åheden*Pinus* to 110.4% in control plots at Wetzstein 35. *Treatment* was a significant source of variation for Åheden*Pinus* ($P < 0.05$), but not for the Wetzstein stands. *Stand age* was not significant for the Wetzstein stands (Table 6).

Table 6. Results of a one-way Anova (Åheden*Pinus*) and a two-way Anova (Wetzstein) for both pM values and flux rates of soil respired CO_2. The source of variance in the one-way Anovas is *treatment* (girdled or control). The sources of variance in the two-way Anovas are *treatment* and *stand age*. Levels of significance are $P < 0.05$ (*) and $P < 0.01$ (**).

	Åheden*Pinus*		Wetzstein	
	pM	Flux	pM	Flux
Source of variation	F	F	F	F
Treatment	9.6*	4.6	1.1	8.2*
Stand age	n.a.	n.a.	2.6	0.0
Interaction	n.a.	n.a.	0.6	0.9

n.a. = not applicable

The contributions of heterotrophic respiration to total soil respiration were calculated using (1) flux rates and (2) pM of soil respired CO_2 (Figure 14). Values ranged from 53% (Åheden*Pinus*, flux approach) to 87% (Wetzstein 35, pM approach) heterotrophic respiration and tended to be higher for the Wetzstein stands than for the Åheden*Pinus* stand. Differences in the calculated fractions of heterotrophic respiration between 10 and 27% were not statistically significant for any of the different stands or approaches. Standard errors ranged from 10% (Åheden*Pinus*, pM approach) to 51% (Wetzstein 35, pM approach). At the Wetzstein stands, standard errors were smaller for the flux approach (13% ≤ SE ≤ 14%) than for the pM approach (34% ≤ SE ≤ 51%). On the contrary, at Åheden*Pinus*, the standard error was smaller for the pM approach (10%) compared to the flux approach (15%). For each stand, the standard deviation of pM was higher in the control plots than in the girdled plots, especially at Wetzstein 114.

Furthermore, I compared pM values of heterotrophically respired CO_2 using three independent models (Table 4). pM values calculated by the cascade model were on average 9.5% (ΔpM) lower than measured in the girdled plots and even lower than pM of atmospheric CO_2. The box model also resulted in lower pM values than measured in the girdled plots (ΔpM 3.4% on average). For the Åheden*Pinus* stand, the modeled pM value of heterotrophically respired CO_2 almost equaled the mean pM value measured on the control plots. For the Wetzstein stands, modeled pM values were lower than those measured on the control plots or even lower than those of atmospheric CO_2. In contrast, pM values calculated by the two-pool model were higher than measured in the girdled plots (ΔpM 4.7% on average) and therefore also higher than pM of CO_2 respired in the control plots. The differences between modeled and measured values (ΔpM) were 3.2% for the Åheden*Pinus* stand, 4.6% for Wetzstein 114 and 6.4% for Wetzstein 35.

Finally, the modeled pM values of heterotrophically respired CO_2 were used to calculate the fractions of heterotrophic respiration relative to total soil respiration (Table 7). For both box and cascade models, calculated values were outside of the defined range (i.e., above 100% or below 0%). The two-pool model resulted in values within the defined range, with lower values than when pM values measured in the girdled plots were used for the calculations. While modeled and measured values differed by 67% (ΔpM) for the Wetzstein 35 stand, fairly good agreement was achieved for the Åheden*Pinus* and the Wetzstein 114 stand, where modeled and measured values differed by 18% and 32% (ΔpM), respectively.

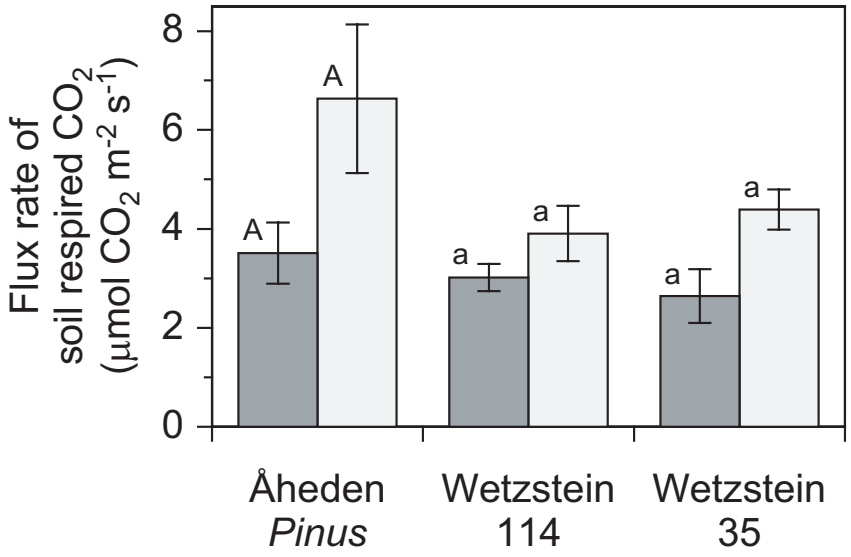

Figure 12. Measured flux rates of soil respired CO_2 (= soil respiration). Dark columns are girdled plots, light columns are control plots. Bars represent standard errors (n = 3; n = 4 for Åheden*Pinus* girdled). Letters indicate statistically significant differences (separately for the Åheden*Pinus* and the Wetzstein stands, $P < 0.05$). Åheden*Pinus* was measured in 2001, Wetzstein in 2002.

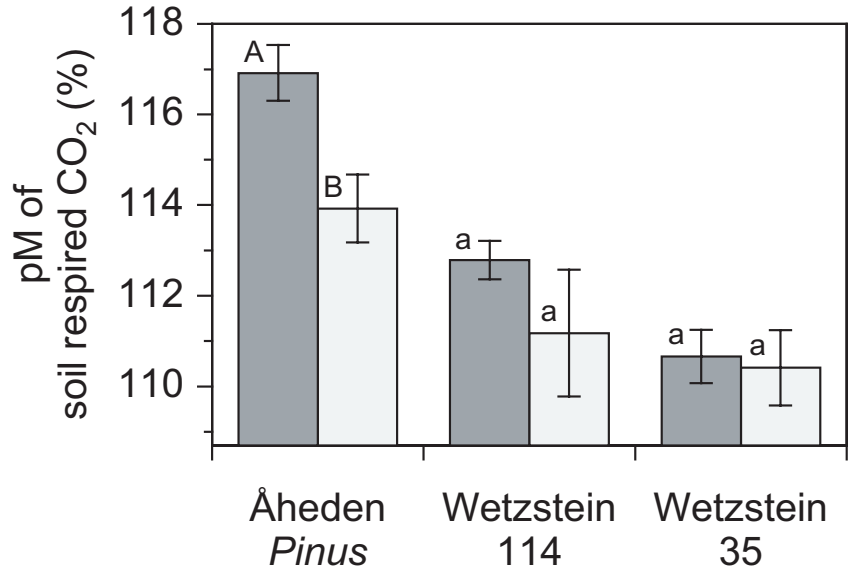

Figure 13. Measured pM (percent Modern) values of soil respired CO_2. Dark columns are girdled plots, light columns are control plots. Bars represent standard errors (n = 3; n = 4 for Åheden*Pinus* girdled). Letters indicate statistically significant differences (separately for the Åheden*Pinus* and the Wetzstein stands, $P < 0.05$). Åheden*Pinus* samples were collected in 2001, Wetzstein samples in 2002. The base line corresponds ± to pM of atmospheric CO_2 (pM = ~108.7%).

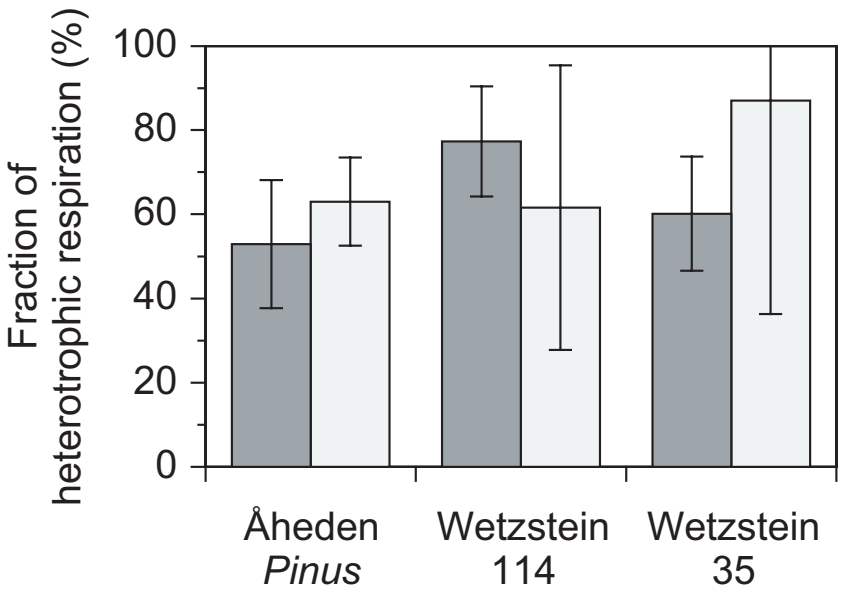

Figure 14. Contributions of heterotrophic soil respiration to total soil respiration calculated by two approaches: (1) Flux rates (dark) and (2) pM values (light) of soil respired CO_2 on girdled and control plots. Bars represent standard errors.

Table 7. Comparison of pM values measured in the girdled plots as well as pM values of heterotrophically respired CO_2 calculated by three models. pM values of autotrophically respired CO_2 and measured pM values of total soil respired CO_2 are given. The fractions of heterotrophic soil respiration relative to total soil respiration were calculated using equation 17 (for more details see text).

	Åheden*Pinus*	Wetzstein 114	Wetzstein 35
	pM of heterotrophically respired CO_2 (%)		
Girdled plots	116.9	112.8	110.7
Box model	113.9	109.3	106.8
Cascade model	102.8	108.0	101.1
Two-pool model	120.1	117.3	117.0
	pM of autotrophically respired CO_2 (%)		
	108.8[#]	108.6[$]	108.7[$]
	pM of total soil respired CO_2 (%)[§]		
	113.9	111.2	110.4
	Fraction of heterotrophic soil respiration (%)		
Girdled plots	63	62	87
Box model	101	348	-88
Cascade model	-85	-420	-22
Two-pool model	45	30	20

[#] measured at atmospheric observation station Jungfraujoch, Swiss Alps, in 2001
[$] measured in-situ on the day of sampling, [§] measured in control plots

3.4 Discussion

Flux rates of soil respired CO_2 in the girdled plots were similar among stands (Figure 12), suggesting that also the flux rates of heterotrophic respiration varied little from stand to stand. On the contrary, flux rates were highly variable among the control plots, in which both autotrophic and heterotrophic respiration contributed to total soil respiration. Therefore, the high variability must have been due to variability in the autotrophic fraction of soil respiration.

The opposite is true for pM of soil respired CO_2. Autotrophically respired CO_2 can be assumed to have a similar pM value at all three stands. Since roots respire recently assimilated carbon (Ekblad and Högberg 2001, Högberg et al. 2001, Horwath et al. 1994), autotrophically respired CO_2 should have a similar pM value as current atmospheric CO_2 (Dörr and Münnich 1986, Wang et al. 2000). pM of atmospheric CO_2, in turn, varies relatively little within Europe (Kromer et al. 2001, Levin and Hesshaimer 2000). In contrast, the pM value of CO_2 respired in the girdled plots varied considerably from stand to stand (Figure 13). These results also suggest that the pM value of heterotrophically respired CO_2 was highly variable among stands.

pM values of soil respired CO_2 were always higher in the girdled plots than in the control plots. The high pM values of CO_2 released from the girdled plots were derived from bomb carbon. The higher the residence time (= turnover time) of active SOC in the soil (up to 20 years), the more ^{14}C enriched is the carbon released by SOC decomposition. This suggests that the residence time of active SOC was highest at Åheden*Pinus*, followed by Wetzstein 114 and Wetzstein 35. These between-stand differences in residence times of active soil organic carbon are only reflected in the pM values of soil respired CO_2 and not in the flux rates.

For several reasons, CO_2 respired in the girdled plots may in fact contain younger (^{14}C depleted) carbon than true heterotrophically respired CO_2 in undisturbed plots. This is because (1) roots of girdled trees may continue to live and respire young starch reserves (Högberg et al. 2001), (2) fine roots may die and feed young carbon to heterotrophs. Moreover, (3) decreased root activity may also decrease the decomposition of relatively old SOC as a result of loss of a positive effect of root exudates on decomposition, so called priming (Kuzyakov et al. 2000). A priming effect was suggested in another study in the Wetzstein 35 stand by Subke et al. (*in review*). Thus, pM of true heterotrophically respired CO_2 may actually be higher than measurements in the girdled plots suggest, as modeled with

the two-pool model (Table 7). This hypothesis is supported by the soil incubations presented in chapter 2, which suggest that modeled pM values of heterotrophically respired CO_2 rather underestimate pM of true heterotrophically respired CO_2. Obviously, the above-mentioned effects also affect flux rates, although in opposite directions, e.g., root respiration resulting from accelerated use of soluble carbohydrates and starch in roots of girdled trees is erroneously interpreted as heterotrophic respiration. Although some uncertainty remains, girdling seems to be the most appropriate method for the experimental separation of heterotrophic and autotrophic respiration at the scale needed in studies of forest ecosystem carbon dynamics.

The fractions of heterotrophic respiration to total soil respiration were calculated using both (1) measured flux rates and (2) pM values of soil respired CO_2 measured in girdled and control plots (Figure 14). Values calculated by both methods agreed well, although standard errors were sometimes large. The standard error of the heterotrophic respiration fraction calculated via pM depends on two variables. First, the differences in pM between girdled and autotrophic as well as between control and autotrophic are critical (Equation 20). These differences were highest for Åheden*Pinus*, which resulted in a low standard error of the heterotrophic respiration fraction. Second, the individual standard errors of pM of soil respired CO_2 in the girdled and control plots are important. For each stand, the standard deviation of pM was higher for the control plots than for the girdled plots. This was probably due to an uneven distribution of active roots in the control plots. The standard error of pM was particularly high for the control plots in the old Wetzstein stand. The reason could be the patchy understory vegetation, which leads to variable proportions of understory autotrophic respiration. In the future, more samples should be taken, especially in the control plots, to minimize the standard error term for the pM approach.

Three different models to calculate pM values of heterotrophically respired CO_2 were tested (Table 7). Both box and cascade models did yield lower pM values than measured in the girdled plots. I believe that this is because both models do not account for the heterogeneity of carbon ages within the soil layers. In fact, each soil layer is composed of carbon with different resident times. Very old pre-bomb carbon, which is low in ^{14}C, has accumulated over time, but hardly contributes to heterotrophic soil respiration. However, in the box and cascade models, all these carbon fractions contribute equally to soil respiration. Physical or chemical fractionations of soil layers are necessary to account for the variable contributions of carbon fractions to heterotrophic soil respiration (Gaudinski et al. 2000, Trumbore and Zheng 1996). Contrary to the box and cascade models, the two-pool model did yield higher

pM values than measured in the girdled plots. Assuming that measurements in the girdled plots underestimate pM, as explained above, pM values calculated by the two-pool model may in fact be a good estimate of true heterotrophically respired CO_2.

Finally, pM values of heterotrophically respired CO_2 calculated by the three models were used to estimate the fractions of heterotrophic soil respiration relative to total soil respiration (Table 7). Both box and cascade models did yield undefined values of either below 0% or above 100%. The reason is that modeled pM values of heterotrophically respired CO_2 were either lower than pM values of autotrophically respired CO_2 or lower than those of CO_2 respired in the control plots. The use of pM values calculated by the two-pool model did yield fractions of heterotrophic soil respiration ranging from 20% (Wetzstein 35) to 45% (Åheden*Pinus*). Although these values were lower than values calculated with pM values measured in the girdled plots, they may be good estimates of the true fractions of heterotrophic respiration in undisturbed plots.

The results show that ^{14}C can be developed to a powerful method to separate the contributions of heterotrophic and autotrophic respiration to total soil respiration. The two-pool model is a promising tool for calculating pM values of heterotrophically respired CO_2, especially where girdling cannot be performed (e.g., non-forest ecosystems or in nature reserves).

4 Isotopic composition of soil CO_2 and soil respired CO_2 in European forests along a latitudinal and two age gradients

4.1 Introduction

Isotopes haven proven to be a useful tool for studying carbon cycling, from the cell to the global level. Carbon and oxygen isotopic compositions (^{13}C, ^{14}C and ^{18}O) of different ecosystem components can be used to quantify the contributions of these components to total ecosystem fluxes (Yakir and Sternberg 2000). The isotopic composition of CO_2-C is strongly determined by its sources. The main sources of soil derived CO_2 are autotrophic respiration, soil organic matter decomposition, and carbonate dissolution. If the isotopic compositions of CO_2 derived from these sources differ, their contributions to soil CO_2 or soil respired CO_2 can be estimated. Note that the term "soil CO_2" denotes CO_2 present in a certain soil depth, while the term "soil respired CO_2" represents CO_2 leaving the soil system at its surface (Amundson et al. 1998).

$\delta^{13}C$ of organic matter and of CO_2 respired from this organic matter (e.g., from litter or roots) varies in time (Buchmann et al. 1997, Schweizer et al. 1999). Variable $\delta^{13}C$ values of assimilated carbon result from changes in source CO_2 for photosynthesis ("Suess effect"; Randerson et al. 2002) and from variations in isotopic discrimination caused by varying ratios of internal (mesophyll airspace) to external (ambient) CO_2 concentrations (Farquhar et al. 1989). These variations are caused by abiotic factors, such as water availability, light supply and nutritional status (Buchmann et al. 1996). The assimilated carbon is transferred to roots and litter. Therefore, changes in $\delta^{13}C$ of soil (respired) CO_2 not only reflect changes in the contributions of CO_2 sources, but also changes in environmental conditions.

Mixing ratios and $\delta^{13}C$ values of soil CO_2 have been combined to calculate $\delta^{13}C$ of soil respired CO_2 using Keeling plots and correcting for a constant diffusive fractionation of 4.4‰ (Cerling and Wang 1996). However, since CO_2 produced in the soil is not evenly(!) enriched in ^{13}C by diffusive fractionation throughout the soil profile, it is questionable whether the Keeling plot approach, which requires two constant endmembers, can be applied to soil CO_2. So far, it has not been tested whether $\delta^{13}C$ values determined by the Keeling plot approach agree with values obtained by other approaches.

As shown in chapter 3, ^{14}C is a valuable tool for partitioning heterotrophic and autotrophic respiration. On sites with limestone bedrock, the dissolution of geogenic (^{14}C free) carbonates may additionally contribute to soil (respired) CO_2 and significantly lower its ^{14}C content. However, the contributions of limestone derived CO_2 to soil (respired) CO_2 have seldom been assessed (Li et al. 2002).

$\delta^{18}O$ of ecosystem respired CO_2 can be used to quantify the contributions of soil derived CO_2 (typically low $\delta^{18}O$ values) and above-ground plant derived CO_2 (typically higher $\delta^{18}O$ values) (Langendörfer et al. 2002, Yakir and Sternberg 2000, Yakir and Wang 1996). CO_2-O in soils is in isotopic exchange with soil H_2O-O (Amundson et al. 1998, Hesterberg and Siegenthaler 1991). The oxygen isotopic composition of soil water, in turn, is influenced by $\delta^{18}O$ of rainwater and in-situ fractionation processes, mainly evapotranspiration (Craig 1961). CO_2 is thought to diffuse out of the soil faster than it can equilibrate with soil water; due to kinetic isotopic fractionation, CO_2 remaining in the soil (i.e., soil CO_2) would become enriched in ^{18}O, relative to its equilibrium value with soil water (Miller et al. 1999, Yakir and Sternberg 2000). Soil CO_2-$\delta^{18}O$ may furthermore be influenced by the invasion of atmospheric CO_2 into the top soil (Stern et al. 2001, Tans 1998). The magnitudes of these different effects, which may all influence soil CO_2-$\delta^{18}O$ values, are still under debate (Riley et al. 2002, Stern et al. 2001).

Although the usefulness of isotopes for studying soil and ecosystem processes has been recognized, data on the isotopic composition of soil respired CO_2 and especially soil CO_2 collected from field studies are still scarce (Amundson et al. 1998).

Thus, the aims of this study were (1) to investigate the spatial and temporal variability of the isotopic composition of both soil CO_2 and soil respired CO_2 in different forest ecosystems throughout Europe, (2) to quantify the different components contributing to soil respiration, (3) to determine the factors (e.g., stand conditions, time of year or stand age) controlling the isotopic composition of soil CO_2, soil respired CO_2 and respiration components, and (3) to compare the Keeling plot approach for determining $\delta^{13}C$ of soil respired CO_2 with a simple chamber method.

4.2 Methods

4.2.1 Sites

Samples of soil CO_2 and soil respired CO_2 were collected from a transect of eight European forest stands from Northern Sweden to Central Italy, and from two chronosequences in Germany, a beech (Leinefelde) and a spruce (Wetzstein) chronosequence, each consisting of four or five stands of different ages. The Wetzstein chronosequence consisted of three stands additional to those listed in Table 1. These additional stands were aged 9, 66 and 67 years, respectively. The stands´ characteristics were the same as for Wetzstein 35 and 114. For the Keeling plot calculations, the alpine Norway spruce stand Renon (46°35´N, 11°26´E, 1720 m asl) was included. All stands were part of the European research project FORCAST; most stands were included in the modeling exercise presented in chapter 2.

4.2.2 Sampling

Gas samples of soil CO_2 were collected via stainless steel tubes (800 mm length, one end (300 mm) perforated, 25.4 mm outer diameter) that were installed in the soil of all stands in autumn 2000 (Figure 11). A soil pit was dug and the tubes were carefully drilled into the soil, keeping the inclination of the tubes parallel to the soil surface. Typically, tubes were installed at 7 and 25 cm soil depth. A stainless steel capillary (ID 0.13 mm) was connected to each tube end. After refilling the soil pit, the capillaries ran from the tube ends to the soil surface. At each stand, tubes were installed and sampled in three replicates. For sampling, pre-evacuated flasks (1 l) were connected to the capillary ends at the soil surface via tubes filled with of $Mg(ClO_4)_2$ (60 mm length, ID 9 mm). The dead volume between flask, $Mg(ClO_4)_2$ and capillary was evacuated with a hand pump prior to sampling. Afterwards, the flask valve was opened for 7 hours to draw in sufficient soil air (approximately 800 mbar l). The small inner diameter (0.13 mm) of the capillary served as a flow restrictor to limit disturbance of the soil air system, but allow mass flow.

Soil respired CO_2 was sampled using the chamber method as described in chapter 3 (Figure 11).

4.2.3 Isotopic units

In this chapter, ^{14}C contents are given as

$$\Delta^{14}C = \left[\frac{A \times \left(\frac{975}{1000 + \delta^{13}C} \right)^2}{A_{abs}} - 1 \right] \times 1000\ ‰, \tag{22}$$

where A is the ^{14}C activity of the sample, A_{abs} is the absolute ^{14}C activity of the international standard (NBS oxalic acid), and $\delta^{13}C$ is the $\delta^{13}C$ value of the sample (Stuiver and Polach 1977). $\Delta^{14}C$ was used instead of pM, because ^{14}C contents of soil CO_2 and soil respired CO_2 are generally given in $\Delta^{14}C$. In this way, the data can be directly compared to literature values. Note that, contrary to pM, $\Delta^{14}C$ of an individual substance does change with time. Here, $\Delta^{14}C$ values are given for the year of sampling. A conversion table can be found in the Appendix.

^{18}O contents are given as

$$\delta^{18}O = \left(\frac{R_{sample}}{R_{standard}} - 1 \right) \times 1000\ ‰, \tag{23}$$

where R_{sample} is the molar $^{18}O/^{16}O$ ratio of the sample and $R_{standard}$ is the molar $^{18}O/^{16}O$ ratio of the international VPDB standard [based on the CG99 scale (CSIRO-AR)].

4.2.4 Analyses, corrections, calculations

Mixing ratios, $\delta^{13}C$ and $\Delta^{14}C$ values of CO_2 were measured as described in chapter 3. The same corrections for the contribution of atmospheric CO_2 to total CO_2 sampled with the chamber method were applied as described in chapter 3.

$\delta^{18}O$ values of CO_2 in equilibrium with rainwater at soil temperature were calculated using the equation given by Yakir and Sternberg (2000):

$$\delta^{18}O_{CO_2} = \delta^{18}O_{water} + \left(\frac{17604}{T} \right) - 17.93, \tag{24}$$

where T is the temperature in Kelvin. The soil temperature at 5-10 cm soil depth was measured with a Licor 6400 temperature probe. Rainwater $\delta^{18}O$ values of the respective areas were taken from IAEA/WMO (2001).

4.2.5 Partitioning of soil respiration

The contributions of heterotrophic respiration to total soil respiration were calculated for those non-limestone stands, where the necessary input data was available. ^{14}C contents of heterotrophically respired CO_2 correspond to modeled pM values of the active pool carbon as described in chapters 2 and 3 (Two-pool model). Fractions of heterotrophic respiration were calculated by the ^{14}C approach as explained in chapter 3. Atmospheric air for $\Delta^{14}C$ analyses was sampled in-situ as explained in chapter 3. Where no atmospheric air samples were taken, either $\Delta^{14}C$ values from the atmospheric observation station Jungfraujoch, Swiss Alps (Ingeborg Levin, University of Heidelberg, *personal communication*) were used or $\Delta^{14}C$ values were derived from the $\Delta^{14}C$ values of the in-situ air sampled in the following year assuming an annual decline of atmospheric $\Delta^{14}C$ by 8‰ as reported by Levin and Kromer (1997):

$$\Delta^{14}C(t) = \Delta^{14}C(t+1) + 8\ ‰, \tag{25}$$

Flux rates of soil respired CO_2 were measured using a LICOR 6400-9 as described in chapter 3.

4.2.6 Keeling plot approach

Using mixing ratios and $\delta^{13}C$ values of soil CO_2, Keeling plots as described by Keeling (1958) were calculated for all stands by geometric mean regression. To account for diffusive fractionation, a constant value of 4.4‰ was subtracted from the intercept to obtain $\delta^{13}C$ of soil respired CO_2 as described by Cerling and Wang (1996):

$$\delta^{13}C_{respired} = \delta^{13}C_{intercept} - 4.4\ ‰ \tag{26}$$

4.3 Results

4.3.1 Spatial variability

Mixing ratios of soil CO_2 increased with depth at all stands of the European transect during summer 2001 (July 29 to September 1) (Figure 15). While some stands showed a more pronounced increase of CO_2 mixing ratios within the top 10 cm (Flakaliden, Sorø), other stands showed an almost linear increase of CO_2 mixing ratios throughout the whole (measured) soil profile (Hesse, Collelongo and Hainich), assuming that the CO_2 mixing ratio

at the soil surface is close to the mixing ratio of atmospheric CO_2. Maximum [CO_2] values were close to 1.1% at Flakaliden (25 cm depth) and Hainich (40 cm depth). Generally, the lowest soil CO_2 mixing ratios were observed at Loobos and Collelongo. CO_2 mixing ratios at similar soil depths varied only little among the three replicates within one stand.

$\delta^{13}C$ values of soil CO_2 ranged from -23.1‰ to -16.7‰ at the European transect stands in summer 2001 (Figure 15). Values typically decreased with soil depth and were negatively correlated with the corresponding CO_2 mixing ratios (see below). $\delta^{13}C$ values of soil respired CO_2 were always lower than those of soil CO_2. Values of soil respired CO_2 ranged from -27.3‰ (Loobos) to -23.0‰ (Collelongo), with standard errors between 0.1‰ and 0.5‰ (Figure 15 and Table 8). The $\delta^{13}C$ value of soil respired CO_2 at Collelongo in summer was at least 2.5‰ higher than at any other stand.

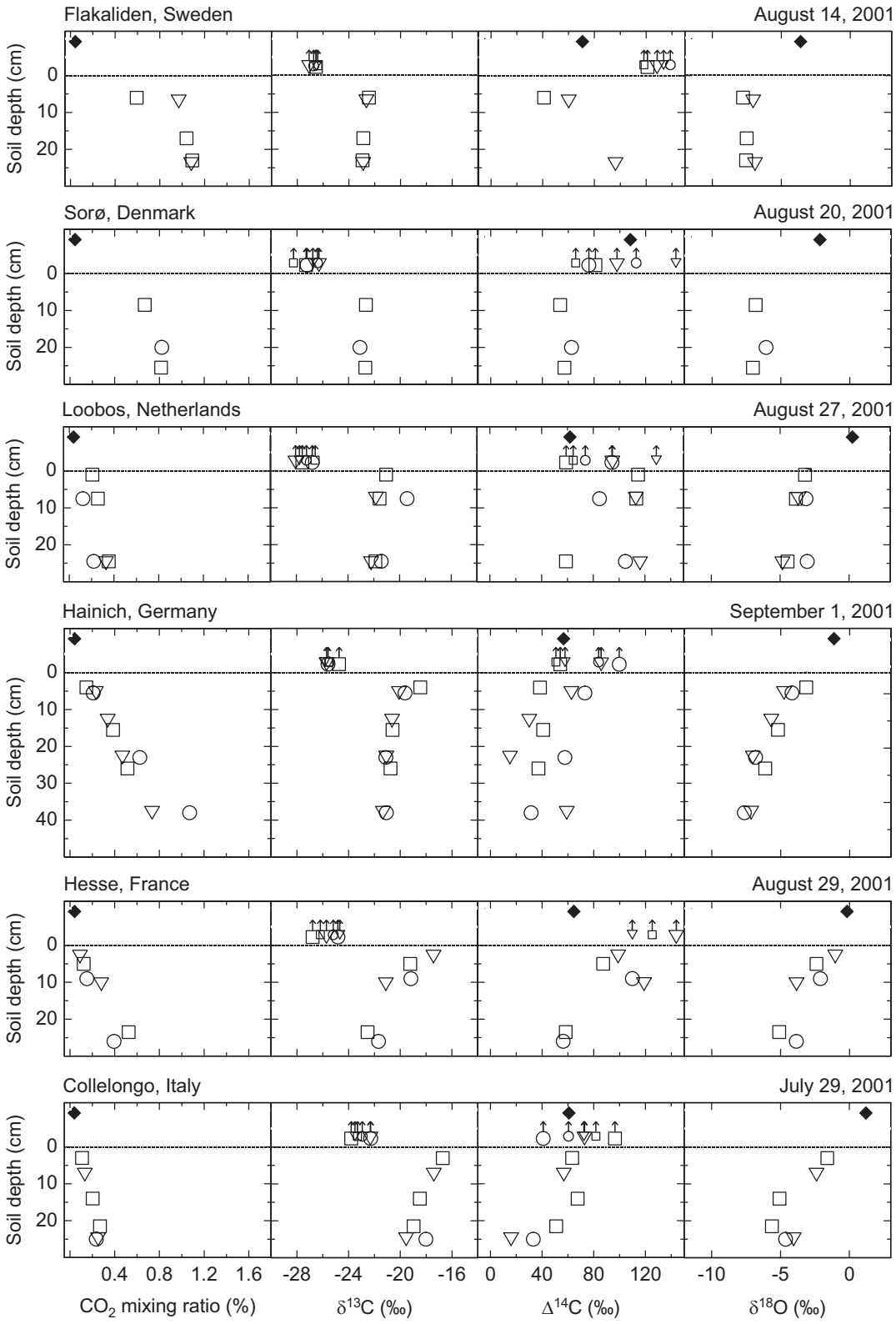

Figure 15. Soil CO_2 and soil respired CO_2 of European forest stands in summer 2001. The symbols triangle, square and circle represent the three sampling locations per site. Symbols combined with an arrow represent soil respired CO_2. Big symbols denote soil respired CO_2 sampled directly above the soil CO_2 tubes, while small symbols indicate soil respired CO_2 sampled approximately 2 m away from the tubes. Filled diamonds represent free air samples. $\delta^{13}C$ values of atmospheric CO_2 were between -11.0‰ and -7.8‰ (not shown).

Table 8. Isotopic signatures of soil respired CO_2 (chamber method). Standard errors (SE) are given.

Site	Date	$\delta^{13}C$ (‰)	SE (‰)	n	$\Delta^{14}C$ (‰)	SE (‰)	n
Flakaliden	14.08.01	-26.7	0.1	3	129.8	5.6	3
Flakaliden	18.-20.10.00	-27.7	0.2	3	76.3	9.8	3
Sorø	20.08.01	-27.0	0.4	3	96.1	13.6	3
Sorø	26.-27.10.00	-28.1	0.1	3	71.9	2.1	3
Loobos	27.08.01	-27.3	0.3	3	85.9	14.5	3
Loobos	31.10.-02.11.00	-27.8	0.4	3	78.8	8.6	3
Hainich	25.03.02	-27.5	0.1	3	81.4	9.0	3
Hainich	07.08.02	-26.1	0.3	3	96.2	10.6	3
Hainich	01.09.01	-25.5	0.2	3	71.9	11.4	3
Hainich	12.-14.12.00	n.a.	n.a.	0	n.a.	n.a.	0
Hesse	29.08.01	-25.6	0.5	3	126.0	0.8	2
Hesse	22.11.00	-28.5	0.4	2	110.1	-	1
Renon	10.-12.11.00	-24.4	0.4	3	130.9	-	1
Collelongo	29.07.01	-23.0	0.3	3	70.8	11.1	3
Collelongo	14.-16.11.00	-25.6	-	1	n.a.	n.a.	0
Leinefelde 30	06.06.01	-26.2	0.6	3	100.5	4.7	3
Leinefelde 62	05.06.01	-26.7	0.5	3	93.5	6.9	3
Leinefelde 111	07.06.01	-27.1	0.2	3	98.6	10.7	2
Leinefelde 153+15	08.06.01	-26.9	0.4	3	87.0	4.9	3
Wetzstein 9	13.06.01	-26.2	0.2	3	87.7	2.9	2
Wetzstein 35	24.07.02	-25.8	0.2	3	97.2	8.2	3
Wetzstein 66	12.07.01	-25.5	0.5	3	110.1	8.1	3
Wetzstein 67	12.06.01	-25.5	0.4	3	110.0	4.7	2
Wetzstein 114	15.06.01	-26.2	0.3	3	124.0	-	1
Wetzstein 114	25.07.02	-26.1	0.2	3	104.8	13.9	3
Åheden*Pinus*	13.08.01	-26.4	0.3	3	132.2	7.5	3

n.a. = not available

$\Delta^{14}C$ values of free air CO_2 in summer 2001 ranged from 56.6‰ (Hainich) to 108.1‰ (Sorø) (Figure 15). Except for Sorø, all free air $\Delta^{14}C$ values were below 82‰, which was the mean $\Delta^{14}C$ value of atmospheric CO_2 measured at the observation station Jungfraujoch, Swiss Alps, in 2001 (Ingeborg Levin, University of Heidelberg, *personal communication*). $\Delta^{14}C$ values of soil CO_2 ranged from 15.1‰ to 118.9‰ and were usually higher at non-limestone stands (i.e., Flakaliden, Loobos and Hesse). Values tended to decrease with soil depth, except at Flakaliden and Sorø. Soil respired CO_2 had higher mean $\Delta^{14}C$ values than free air CO_2 at all stands except at Sorø. $\Delta^{14}C$ values of soil respired CO_2 were generally higher than those of soil CO_2 from larger depths, while they were closer to those of soil CO_2 near the soil surface (exceptions: Flakaliden, Sorø). Mean values of $\Delta^{14}C$ of soil respired CO_2 ranged from 70.8‰ (Collelongo) to 129.8‰ (Flakaliden) and tended to be higher at non-limestone stands (Table 8).

For six non-limestone stands, the contributions of heterotrophic respiration to total soil respiration were calculated using the two-pool model (Table 9). Values ranged from only 6%

heterotrophic respiration at Loobos in autumn to a maximum number of 82% at Flakaliden in summer. The mean value across all sites and sampling times was 42%. Fractions of heterotrophic respiration tended to decrease from spring to summer and from summer to autumn. At Loobos and Wetzstein 114, absolute values of autotrophic soil respiration were highest during summer. This agrees with flux rate measurements from the girdling experiments (chapter 3) (Buchmann et al., *in preparation*). High flux rates of autotrophic CO_2 were calculated for the two pine stands, Loobos and Åheden*Pinus*. The two northern stands Flakaliden and Åheden*Pinus*, but also Hesse, the only beech stand, showed high heterotrophic respiration fluxes.

$\delta^{18}O$ values of soil CO_2 ranged from -7.8‰ (Flakaliden) to -1.0‰ (Hesse) (Figure 15). They showed continuous trends with soil depth. Either values decreased with depth (Loobos, Hainich, Hesse, Collelongo) or they remained constant with depth (Flakaliden, Sorø). $\delta^{18}O$ values of soil CO_2 at 5-10 cm depth were compared with those of CO_2 in equilibrium with rainwater at soil temperature (Figure 16). Rainwater $\delta^{18}O$ values were taken from IAEA/WMO (2001). Soil CO_2 was enriched in ^{18}O compared to those of rainwater CO_2 by on average 0.4‰ ($\Delta\delta^{18}O$). These enrichments were most pronounced in samples taken in October/November.

Table 9. Shown are $\Delta^{14}C$ values of heterotrophically respired CO_2 calculated with the two-pool model, $\Delta^{14}C$ values of autotrophically respired CO_2 and $\Delta^{14}C$ values of total soil respired CO_2. The fractions of heterotrophic soil respiration relative to total soil respiration were calculated by combination of the shown $\Delta^{14}C$ values (equation 17, chapter 3). Absolute flux rates of hetero- and autotrophic respiration were calculated by multiplying respiration fractions and total measured flux rates. The precision of $\Delta^{14}C$ is about 7‰.

	Flakaliden	Loobos	Hesse	Åheden*Pinus*	Wetzstein 114	Wetzstein 35
Modeled $\Delta^{14}C$ of heterotrophically respired CO_2 (‰)						
	143.0	209.0	143.6	194.1	166.0	163.2
$\Delta^{14}C$ of autotrophically respired CO_2 (‰)[A]						
Spring 2001	-	-	-	-	87.1[C]	-
Summer 2001 & 2002	70.7[B]	62.0[B]	64.5[B]	81.6[D]	79.1[B]	80.6[B]
Autumn 2000	78.7[C]	70.0[C]	72.5[C]	-	-	-
$\Delta^{14}C$ of total soil respired CO_2 (‰)						
Spring 2001	-	-	-	-	124.0	-
Summer 2001 & 2002	129.8	85.9	126.0	132.2	104.8	97.2
Autumn 2000	76.3	78.8	110.1	-	-	-
Fraction of heterotrophic soil respiration (%)						
Spring 2001	-	-	-	-	47	-
Summer 2001 & 2002	82	16	78	45	30	20
Autumn 2000	n.d.	6	53	-	-	-
Flux rates of soil respired CO_2 ($\mu mol\ m^{-2}s^{-1}$) [heterotrophic / autotrophic]						
Spring 2001	-	-	-	-	1.6 / 1.9	-
Summer 2001 & 2002	5.5 / 1.2	0.8 / 4.0	2.2 / 0.6	3.0 / 3.6	1.2 / 2.7	0.9 / 3.5
Autumn 2000	-	0.1 / 2.0	1.3 / 1.1	-	-	-

[A] derived from atmospheric measurements
[B] atmospheric air sampled in-situ
[C] derived from in-situ sample of the following year [$\Delta^{14}C(t) = \Delta^{14}C(t+1) + 8‰$]
[D] measured at atmospheric observation station Jungfraujoch, Swiss Alps
n.d. = not defined

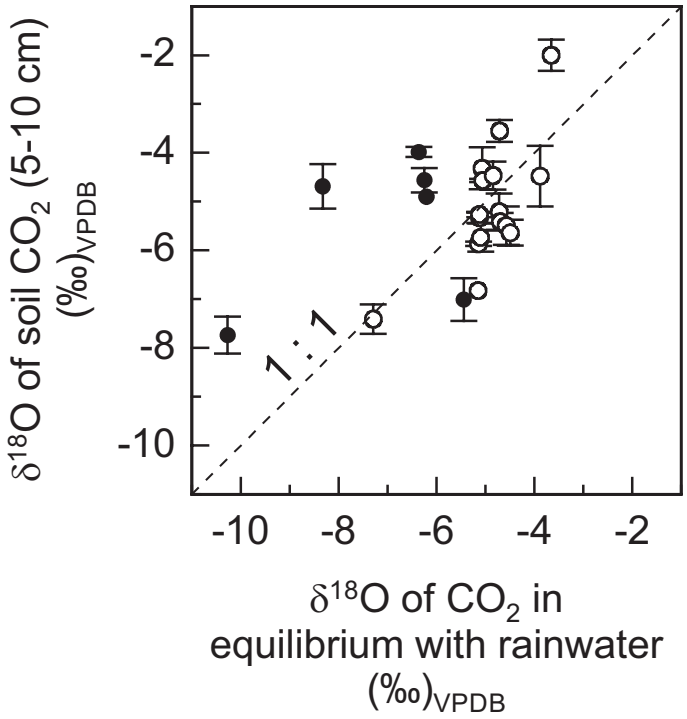

Figure 16. Relationship between $\delta^{18}O$ of soil CO_2 in 5-10 cm soil depth and $\delta^{18}O$ of CO_2 in equilibrium with rainwater at soil temperature. Filled symbols represent soil CO_2 samples taken in October and November, while open symbols represent samples taken in March, June, July or August. Rainwater data was taken from IAEA/WMO (2001). Bars indicate standard errors.

4.3.2 Seasonal variability

At the Hainich stand, mixing ratios as well as $\delta^{13}C$ values of soil CO_2 showed similar patterns with depth throughout the year (Figure 17). In December, the spatial variability of [CO_2] and $\delta^{13}C$ among the three replicates within one stand was much larger than at any other sampling date. $\delta^{13}C$ values of soil respired CO_2 increased at the Hainich stand from -27.5‰ in March to -26.1‰ in August and -25.5‰ in September (Figure 18A). $\Delta^{14}C$ values of soil respired CO_2 at the Hainich stand increased from March (81.4‰) to August (96.2‰) and sharply decreased from August to September (71.9‰) (Figure 18B). $\delta^{18}O$ values of soil CO_2 at the Hainich stand showed quite variable patterns throughout the year (Figure 17). While $\delta^{18}O$ did not change with depth in March and December, it decreased with depth in August and September.

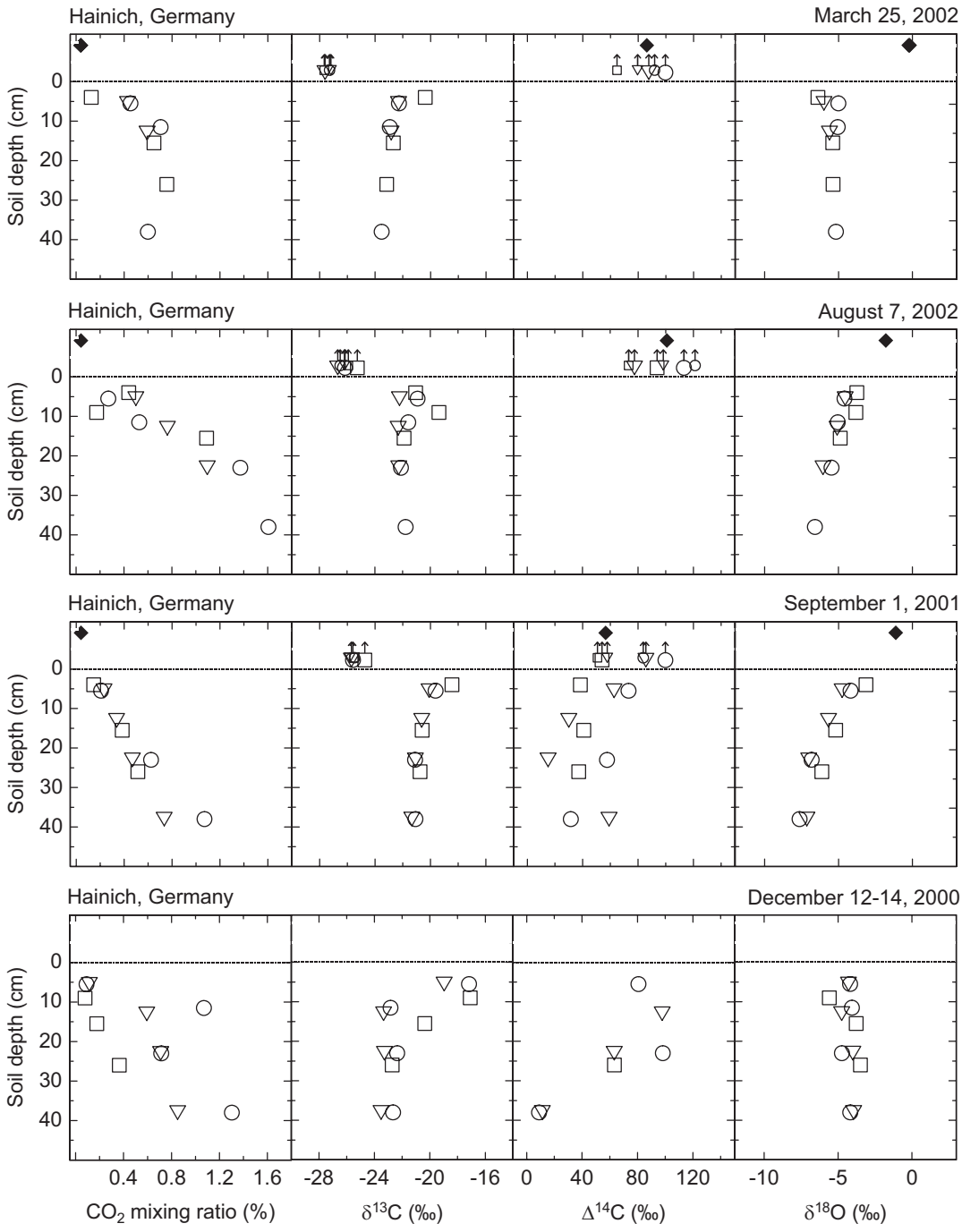

Figure 17. Seasonal change of soil CO_2 and soil respired CO_2 at the Hainich stand. The symbols triangle, square and circle represent the three sampling locations per stand. Symbols combined with an arrow represent soil respired CO_2. Big symbols denote soil respired CO_2 sampled directly above the soil CO_2 tubes, while small symbols indicate soil respired CO_2 sampled approximately 2 m away from the tubes. Filled diamonds represent free air samples. $\delta^{13}C$ values of free air CO_2 were between -11.1‰ and -8.7‰ (not shown).

At Wetzstein 114, $\delta^{13}C$ values of soil respired CO_2 were quite constant from June to July (-26.1‰; Figure 18A). All other stands showed decreasing $\delta^{13}C$ values from July/August to October/November. $\Delta^{14}C$ values decreased from June (124.0‰) to July (105.0‰) at Wetzstein 114. At all other stands, $\Delta^{14}C$ values decreased from July/August to October/November.

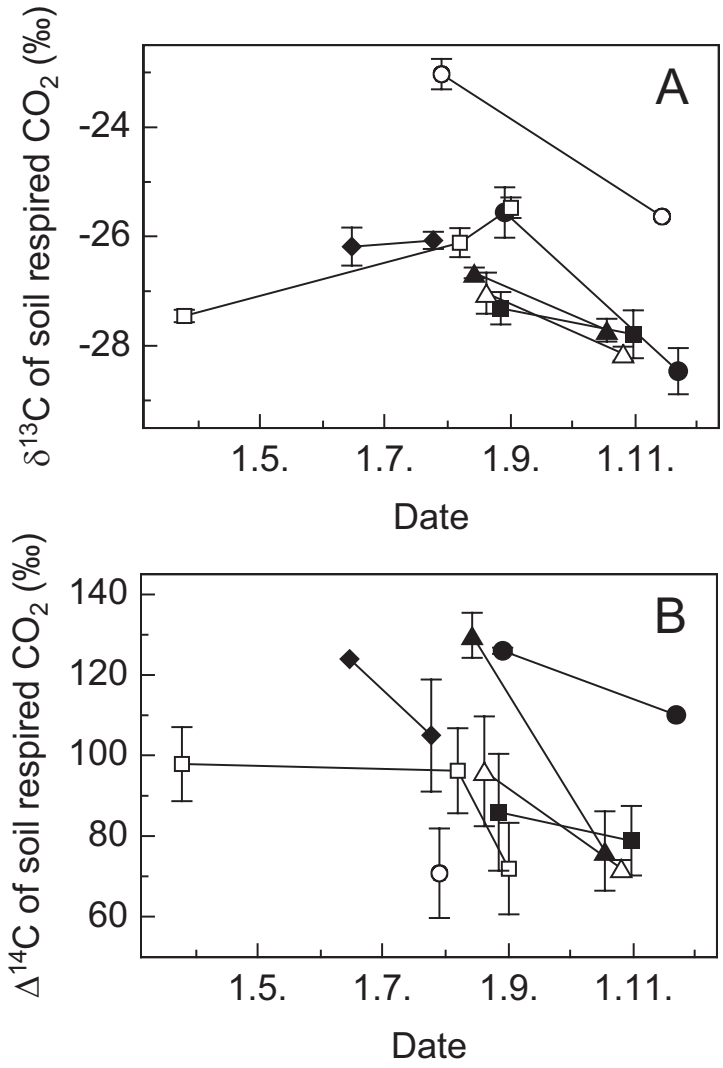

Figure 18. Seasonal course of $\delta^{13}C$ (A) and $\Delta^{14}C$ (B) of soil respired CO_2 from March 2002 to December 2000. Bars indicate standard errors. Stands on limestone have open symbols. Flakaliden (filled triangles), Sorø (open triangles), Loobos (filled squares), Hainich (open squares), Hesse (filled circles), Collelongo (open circles) and Wetzstein 114 (filled diamonds).

4.3.3 Age effects

Comparing mean soil CO_2 mixing ratios, similar trends of increasing [CO_2] with depth were observed at all four stands of the beech chronosequence in Leinefelde, independent of stand age (Figure 19). Mean $\delta^{13}C$ values of soil CO_2 ranged from -23.3‰ to -21.6‰ at all depths in Leinefelde. I found similar trends of soil CO_2 $\delta^{18}O$ values, which decreased with depth at all Leinefelde chronosequence stands (Figure 19).

$\delta^{13}C$ values of soil respired CO_2 decreased from Leinefelde 30 (-26.2‰) to Leinefelde 111 (-27.1‰), and slightly increased from Leinefelde 111 to Leinefelde 153+15 (-26.9‰) (Figure 20A). Such a trend could not be found for the Wetzstein spruce chronosequence (Figure 20B). $\Delta^{14}C$ values of soil respired CO_2 increased linearly with stand age at the Wetzstein chronosequence (R^2 = 0.991, P = 0.005), while no consistent trend of $\Delta^{14}C$ with stand age was found for the Leinefelde chronosequence.

4.3.4 Keeling plot approach

Mixing ratios and $\delta^{13}C$ values of soil CO_2 were used to calculate $\delta^{13}C$ of soil respired CO_2 with the Keeling plot approach as described by Keeling (1958). To account for diffusive fractionation in the soil, a constant value of 4.4‰ ($\Delta\delta^{13}C$) was subtracted from the calculated intercept (Cerling and Wang 1996). The results showed that in 18 out of 22 cases, the Keeling plot approach underestimated $\delta^{13}C$ of soil respired CO_2 as compared to the chamber method (Table 10). In three of the four cases, where the Keeling plot approach yielded higher values, R^2 was clearly below 0.9.

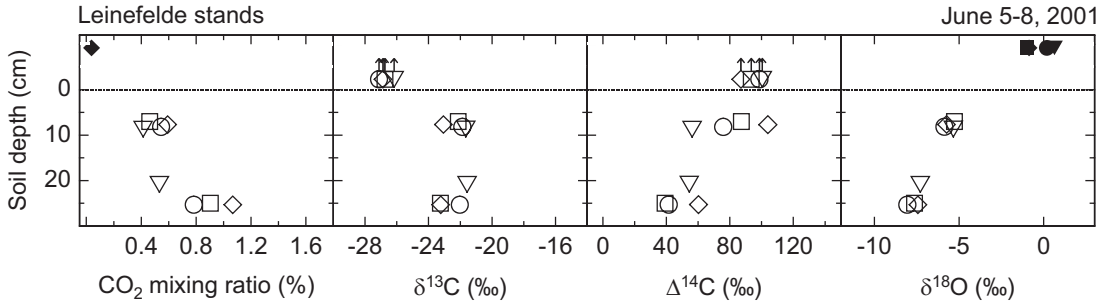

Figure 19. Soil CO_2 and soil respired CO_2 of the Leinefelde beech chronosequence stands. Triangle = Leinefelde 30, square = Leinefelde 62, circle = Leinefelde 111, diamond = Leinefelde 153+15. Symbols combined with an arrow represent soil respired CO_2. Filled diamonds represent free air samples. $\delta^{13}C$ values of free air CO_2 were between -11.0‰ and -8.3‰ (not shown).

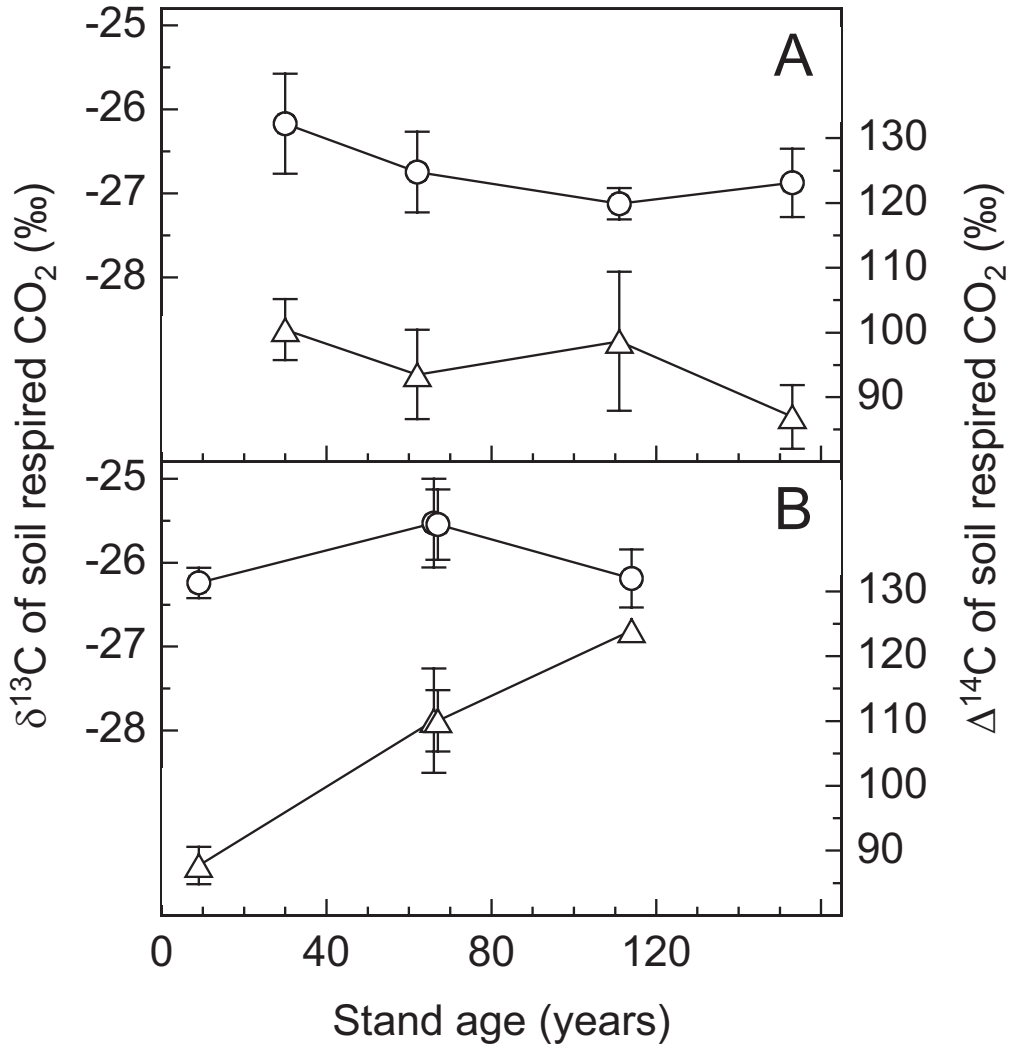

Figure 20. Relationships of $\delta^{13}C$ (circles) and $\Delta^{14}C$ (triangles) of soil respired CO_2 and stand age for the Leinefelde beech (A) and Wetzstein spruce (B) chronosequences in June/July 2001. Bars indicate standard errors. Note that the oldest stand at Leinefelde had an understory of approximately 15-year-old beech trees. The 66-year-old spruce stand at Wetzstein was sampled approximately 40 days after the other stands. At the Wetzstein, $\Delta^{14}C$ of soil respired CO_2 increased linearly with stand age ($y = 0.35x + 85.7$, $R^2 = 0.991$, $P = 0.005$)

Table 10. Comparison of $\delta^{13}C$ values of soil respired CO_2 calculated by two different approaches. Standard deviations (SD) are given. For the Keeling plot approach, n is the number of soil CO_2 data points (from all three sampling locations); for the chamber method, n is the number of sampling locations within one stand. $\Delta\delta^{13}C$ is the difference between the $\delta^{13}C$ values from the two approaches.

Site	Date	R^2	$\delta^{13}C$ (‰)	SD (‰)	n	$\delta^{13}C$ (‰)	SD (‰)	n	$\Delta\delta^{13}C$ (‰)
		Keeling plot method				Chamber method			
Flakaliden	14.08.01	1.000	-27.8	0.0	6	-26.7	0.2	3	-1.1
Flakaliden	18.-20.10.00	0.986	-27.2	0.2	6	-27.7	0.4	3	0.5
Sorø	20.08.01	0.999	-28.0	0.1	4	-27.0	0.7	3	-1.0
Sorø	26.-27.10.00	0.865	-27.9	0.2	6	-28.1	0.2	3	0.2
Loobos	27.08.01	0.998	-28.4	0.1	8	-27.3	0.5	3	-1.1
Loobos	31.10.-02.11.00	0.663	-27.5	1.6	6	-27.8	0.8	3	0.3
Hainich	25.03.02	0.996	-28.4	0.2	11	-27.4	0.2	3	-0.9
Hainich	07.08.02	0.998	-27.0	0.1	13	-26.1	0.5	3	-0.9
Hainich	01.09.01	0.998	-26.4	0.1	12	-25.5	0.3	3	-0.9
Hainich	12.-14.12.00	0.964	-28.2	0.2	11	n.a.	n.a.	0	n.a.
Hesse	29.08.01	0.984	-27.9	0.3	8	-25.6	0.8	3	-2.3
Hesse	22.11.00	0.978	-29.9	0.4	4	-28.5	0.6	2	-1.4
Renon	10.-12.11.00	0.542	-26.4	0.5	6	-24.4	0.8	3	-2.0
Collelongo	29.07.01	0.988	-25.3	0.2	7	-23.0	0.5	3	-2.3
Collelongo	14.-16.11.00	0.525	-25.5	0.7	6	-25.6	-	1	0.1
Leinefelde 30	06.06.01	0.995	-27.5	0.2	7	-26.2	1.0	3	-1.3
Leinefelde 62	05.06.01	0.997	-28.1	0.1	7	-26.7	0.8	3	-1.4
Leinefelde 111	07.06.01	0.997	-27.2	0.1	8	-27.1	0.3	3	-0.1
Leinefelde 153+15	08.06.01	0.988	-28.4	0.3	7	-26.9	0.7	3	-1.5
Wetzstein 9	13.06.01	0.997	-28.0	0.1	8	-26.2	0.3	3	-1.8
Wetzstein 66	12.07.01	0.998	-26.6	0.1	7	-25.5	0.9	3	-1.1
Wetzstein 67	12.06.01	0.952	-26.6	0.2	6	-25.5	0.7	3	-1.1
Wetzstein 114	15.06.01	0.791	-27.4	0.3	6	-26.2	0.6	3	-1.2
Wetzstein 114	25.07.02	n.a.	n.a.	n.a.	0	-26.1	0.3	3	n.a.

n.a. = not available

4.4 Discussion

4.4.1 Spatial variability

Mixing ratios of soil CO_2 reflect both CO_2 production and gas diffusivity in the soil. The two stands Collelongo and Loobos showed particularly low soil CO_2 mixing ratios throughout the profiles (Figure 15). Soils at both stands probably have a high gas diffusivity due to near-surface limestone at Collelongo and coarse sand in Loobos. Contrary, Flakaliden and Hainich showed the highest CO_2 mixing ratios. The soil at the Hainich site is rich in clay and probably less diffusive for gases. Since the sandy soil at the Flakaliden site should have a good gas diffusivity, high soil CO_2 mixing ratios are probably the result of high CO_2 production in the soil. The almost linear relationship of CO_2 mixing ratio with depth (as observed at most stands) indicates decreasing soil diffusivity with depth. This may be have been due to several causes, e.g., less perturbations by soil fauna, less aggregates, less root canals or increased soil moisture in deeper depths. Linear profiles may also indicate high CO_2 production in larger soil depths. Contrary, the non-linear profiles (Flakaliden and Sorø) indicate that soil diffusivity did not decrease with depth or that proportionally more CO_2 was produced closer to the soil surface. The latter appears to be an appropriate explanation for the Flakaliden stand, which is nitrogen limited and where, presumably, most roots grow and respire in the top centimeters of the soil, where most nitrogen is available.

Soil CO_2 is a mixture of CO_2 produced in the soil and atmospheric CO_2. $\delta^{13}C$ values and mixing ratios of soil CO_2 were negatively correlated, mainly due to an increasing proportion of (isotopically light) CO_2 produced in the soil with increasing CO_2 mixing ratio. Later in this discussion, the possibility is assessed to use this fact for calculating $\delta^{13}C$ of soil respired CO_2 by applying a Keeling plot to mixing ratios and $\delta^{13}C$ values of soil CO_2. In summer, $\delta^{13}C$ values of soil respired CO_2 were much higher at Collelongo (-23.0‰) than at all other stands. The plants at Collelongo obviously suffer from water stress in summer. Water stress causes stomatal closure, which reduces isotopic discrimination during photosynthesis (Farquhar et al. 1989). Since recently assimilated photosynthates are the major source for autotrophic respiration (Horwath et al. 1994, Högberg et al. 2001), high $\delta^{13}C$ values of soil respired CO_2 reflect the low water availability at Collelongo in summer. A close relationship between moisture conditions and $\delta^{13}C$ of soil respired CO_2 was also found by Ekblad and Högberg (2001).

$\Delta^{14}C$ values of free air CO_2 varied from stand to stand and tended to be lower than the mean value measured at the atmospheric observation station in Jungfraujoch, Swiss Alps (Ingeborg Levin, University of Heidelberg, *personal communication*). The low values can partly be explained by mixing of fossil fuel derived CO_2, but it appears questionable, whether this can completely explain the low values observed, especially for sites far away from industrial regions (e.g., Flakaliden). A second reason for the descrepancies may be that atmospheric observation stations integrate day- and night-time CO_2. However, night-time CO_2 might be enriched in ^{14}C due to a higher proportion CO_2 derived from soil respiration (Susan E. Trumbore, University of California, Irvine, USA, *personal communication*). In the future, more attention should be paid to local and temporal deviations from mean atmospheric ^{14}C contents.

$\Delta^{14}C$ values of soil CO_2 were lowest at Sorø, Hainich and Collelongo. All these stands have limestone bedrock. Probably, CO_2 from the dissolution of geogenic carbonate contributed to soil CO_2. Geogenic carbonate is ^{14}C free and has a $\Delta^{14}C$ value of –1000‰. Therefore, a small proportion of only 1% carbonate derived CO_2 would lead to a decrease of mean CO_2-$\Delta^{14}C$ by 10 to 12‰ ($\Delta\Delta^{14}C$), depending on the ^{14}C content of CO_2 from heterotrophic plus autotrophic respiration. A contribution of carbonate derived CO_2 to soil CO_2 is also indicated by decreasing $\Delta^{14}C$ values with depth, as carbonate dissolution is assumed to occur mainly in larger soil depths. However, also non-carbonate soils tended to have decreasing $\Delta^{14}C$ values of soil CO_2 with depth. This must have been due to a higher proportion of old, pre-bomb CO_2-C in larger soil depths. This agrees with many studies that have found decreasing $\Delta^{14}C$ values of soil organic carbon with depth (e.g., Baisden et al. 2002, Chen et al. 2002, O'Brien and Stout 1978, Pessenda et al. 2001, Torn et al. 2002, Trumbore 2000, Wang et al. 1999). Similar to soil CO_2, also soil respired CO_2 seemed to contain proportions of carbonate derived CO_2 on limestone sites, indicated by low $\Delta^{14}C$ values. On average, soil respired CO_2 on the three limestone sites was depleted in ^{14}C by 34‰ ($\Delta\Delta^{14}C$) compared to non-limestone sites. This corresponds to a contribution of carbonate derived CO_2 to total soil respired CO_2 of approximately 3%. While few such numbers can be found in the literature (Li et al. 2002), these estimates can help to assess weathering rates and nutrient release from bedrock.

$\Delta^{14}C$ values of soil respired CO_2 were usually closer to soil CO_2 nearer to the surface than to those at large depths, suggesting that most CO_2 was produced in the upper centimeters of the soil.

At all non-limestone sites, $\Delta^{14}C$ values of soil respired CO_2 were higher than $\Delta^{14}C$ values of atmospheric CO_2. This agrees with the results of chapter 2 and 3 and confirms that CO_2 produced by heterotrophic respiration is enriched in ^{14}C compared to autotrophically respired CO_2. Fractions and flux rates of heterotrophic and autotrophic respiration calculated using the two-pool model tended to depend on latitude and tree species. While heterotrophic respiration was high for the northern stands and the beech stand, autotrophic respiration was high for the pine stands. However, more forest stands need to be investigated to confirm these trends.

Soil CO_2-O is in isotopic exchange with soil H_2O-O. Rainwater is believed to be the most important environmental control on the oxygen isotopic composition of soil CO_2 (Amundson et al. 1998, Miller et al. 1999, Mortazavi and Chanton 2002, Riley et al. 2002, Stern et al. 2001, Yakir and Sternberg 2000). Besides rainwater, three main factors determine the oxygen isotopic composition of soil CO_2: (1) Soil water can become enriched in ^{18}O compared to rainwater by evapotranspiration, which, in turn, also increases $\delta^{18}O$ of soil CO_2 (Craig 1961). (2) If CO_2 diffuses out of the soil faster than it can equilibrate with soil water, soil CO_2 becomes isotopically enriched by diffusive kinetic fractionation (Miller et al. 1999, Yakir and Sternberg 2000). (3) Invasion of atmospheric CO_2 into the soil can change $\delta^{18}O$ of soil CO_2 (Stern et al. 2001, Tans 1998). Since atmospheric CO_2 is usually enriched in ^{18}O compared to soil CO_2, this process increases $\delta^{18}O$ of soil CO_2. Therefore, all three processes increase $\delta^{18}O$ of soil CO_2 in relation to $\delta^{18}O$ of CO_2 in equilibrium with rainwater. However, the results suggest that in some cases, $\delta^{18}O$ of soil water closer to the soil surface was depleted in ^{18}O compared to $\delta^{18}O$ of rainwater (Figure 16). Rainwater $\delta^{18}O$ data were taken from IAEA/WMO (2001) and represent averages over large areas. Therefore, in specific cases, data taken from these maps may under- or overestimate $\delta^{18}O$ values of rainwater at any specific stand. On average, soil CO_2 in 5 to 10 cm depth was enriched in ^{18}O compared to CO_2 in equilibrium with rainwater by a mean value of 0.4‰ ($\Delta\delta^{18}O$). Furthermore, the enrichments in ^{18}O were most pronounced in October/November. This indicates that invasion of atmospheric CO_2 is the major process responsible for the ^{18}O enrichments. Both evapotranspiration and diffusive fractionation are expected to be more pronounced in the summer, when the soil is drier and more CO_2 is produced in the soil. Contrary, the invasion effect is expected to be highest in winter, when (1) atmospheric CO_2 mixes with lower mixing ratios of CO_2 produced in the soil, and (2) the oxygen isotopic difference between atmospheric CO_2 and CO_2 in equilibrium with rainwater is highest.

However, oxygen isotopic enrichment by evapotranspiration may at some stands have played an important role during summer. This is indicated by decreasing values of soil CO_2-$\delta^{18}O$

with depth at Loobos, Hesse and Collelongo (Figure 15). Also at the Hainich stand, decreasing summer values of soil CO_2-$\delta^{18}O$ with depth indicate isotopic fractionation of top soil water due to evapotranspiration (Figure 17). This trend was not observed in March and December, when soil CO_2-$\delta^{18}O$ values were constant with depth. Also at Flakaliden and Sorø, soil CO_2-$\delta^{18}O$ values were constant with depth, indicating that no isotopic fractionation of soil water did occur.

4.4.2 Seasonal variability

At all stands, $\delta^{13}C$ values of soil respired CO_2 were highest in summer (Figure 18A). This was probably due to decreased water availability during summer. Dry conditions lead to decreasing discrimination against the heavy isotope ^{13}C during photosynthesis, which is reflected in higher $\delta^{13}C$ values of soil respired CO_2 (Ekblad and Högberg 2001, Farquhar et al. 1989). Changes in time of soil respired CO_2-$\Delta^{14}C$ may have different causes. Low $\Delta^{14}C$ values of soil respired CO_2 in October/November at Sorø and Collelongo may have been caused by a higher fraction of CO_2 derived from geogenic carbonates. Also, the contributions of heterotrophically and autotrophically respired CO_2 to total soil respired CO_2 may vary in time (Janssens et al 2003b, Wang et al. 2000). My model calculations suggest that the proportions of heterotrophically respired CO_2 decreased from August/September to October/November at the stands Flakaliden, Loobos and Hesse. This contradicts results from a girdling experiment at Åheden*Pinus*, where the fractions of heterotrophic respiration were lowest in summer (Högberg et al. 2001). At Wetzstein 114, the contribution of heterotrophically respired CO_2 decreased from June to July. This agrees well with flux data from the girdling experiment, which showed that the proportion of heterotrophic respiration is lowest in summer (Buchmann et al., *in preparation*, Subke et al., *in review*). Another explanation could be that the microbial community decomposes substrates of different ages and ^{14}C contents in summer and autumn. This would cause changing $\Delta^{14}C$ values of heterotrophically respired CO_2, a hypothesis that would need to be tested.

4.4.3 Age effects

At the Leinefelde chronosequence, $\delta^{13}C$ values of soil respired CO_2 decreased with stand age from Leinefelde 30 to Leinefelde 111 (Figure 20A). This corresponds to an observed increase of understory vegetation leaf area indices from Leinefelde 30 to Leinefelde 111 (Gerhard Gebauer, University of Bayreuth, *personal communication*). Generally, understory vegetation

has low $\delta^{13}C$ values, which should be reflected in their mycorrhizal root respiration and this could explain the differences in $\delta^{13}C$ of soil respired CO_2 with stand age at the Leinefelde chronosequence. At Leinefelde, the stands with different ages showed very similar $\delta^{18}O$ values of soil CO_2, indicating similar soil hydrological conditions across all stand ages (Figure 19).

While $\Delta^{14}C$ values of soil respired CO_2 showed no consistent trend at Leinefelde, $\Delta^{14}C$ values clearly increased with stand age at the Wetzstein chronosequence (Figure 20B). This was probably due to an increasing fraction of heterotrophic respiration with stand age and agrees with modeled respiration fractions at the two girdling stands (Table 9).

4.4.4 Keeling plot approach

Keeling plots seem to systematically underestimate $\delta^{13}C$ of soil respired CO_2 (Table 10). The Keeling plot approach requires two constant endmembers. In the case of soil CO_2, the two endmembers are atmospheric CO_2 and CO_2 produced in the soil. However, CO_2 produced in the soil is not constant, but - due to diffusive fractionation - is increasingly(!) enriched in ^{13}C with soil depth. Therefore, the relation of $\delta^{13}C$ to the inverse of the respective mixing ratio is not linear, violating the Keeling plot assumptions. As a result, the Keeling plot intercept is less than the predicted 4.4‰ higher than the $\delta^{13}C$ value of soil respired CO_2, due to the inclusion of soil CO_2 from the upper soil, which is less than 4.4‰ enriched in ^{13}C by diffusive fractionation. Thus, subtracting 4.4‰ from the intercept will lead to underestimates in $\delta^{13}C$ of soil respired CO_2. In addition, $\delta^{13}C$ of CO_2 produced in the soil may decrease with depth due to a higher fraction of CO_2 respired from old SOC, which is depleted in ^{13}C, but contributes little to total soil respiration (“Suess effect”; Randerson et al. 2002).

5 Concluding discussion

In this study, I tackled two major challenges of carbon cycle research. The first challenge was to elucidate the amounts and turnover times of active soil organic carbon and to use this information for answering the question to what extent soils can sequester carbon and thereby buffer the accumulation of CO_2 in the atmosphere (chapter 2). The second major challenge was to partition soil respiration into its heterotrophic and autotrophic components (chapters 3 and 4). An additional task was to elucidate and explain patterns of the isotopic composition (^{13}C, ^{14}C and ^{18}O) of soil CO_2 and soil respired CO_2 (chapter 4). Investigations were performed for a variety of European forests across a latitudinal gradient, including two chronosequences.

Major uncertainties exist about the potential of soils for carbon sequestration. On short to intermediate time scales, only the active fraction of SOC can sequester significant amounts of carbon. Consequently, within this study, a new model ("two-pool model") was developed for calculating the turnover time of the active soil organic carbon pool (chapter 2). In addition to the turnover time, the two-pool model also yields the amount of this active carbon, which is distributed throughout the soil profile and which cannot be determined by older models. The amount of active soil carbon can provide important information about soil carbon dynamics and soil carbon sequestration potential (see below). The two-pool model overcomes major deficiencies of older models, particularly in constraining the ^{14}C content of carbon entering and leaving SOC. Using soil incubation experiments, the new model was successfully validated. While the two-pool model offers major advantages over older models, it does require the amount of litter production as an additional input variable.

The model calculations of chapter 2 clearly demonstrate that soils can sequester carbon and thereby increase the amount of organic carbon stored in soils. However, the potential magnitude of soil carbon sequestration is much lower than some of the numbers discussed in the prevailing literature, i.e., clearly below 1 t C ha^{-1} yr^{-1}. Provided that carbon is not eroded from the soil or imported from other soils, soil carbon sequestration depends on two variables only: (1) The amount of carbon input into SOC and (2) the rate at which this SOC turns over. There is a large uncertainty about how SOC turnover may change under shifting climatic conditions. Using the new two-pool model, patterns of active pool turnover were identified for a large number of European forest soils. Turnover times varied by a factor of more than four, but no clear relationship with climatic or geographic variables such as mean annual temperature (MAT), rainfall, nitrogen deposition, soil carbon stocks or latitude could be

found. This contradicts other studies, which revealed decreasing SOC turnover times with increasing mean annual temperatures over a wider range of temperatures (Giardina and Ryan 2000, Raich and Schlesinger 1992, Sanderman et al. 2003, Trumbore et al. 1996). In contrast, soil respiration rates did not increase in a boreal forest after the soil temperature was experimentally increased by a constant offset of 5 °C compared to the control (Strömgren 2001). Possibly, daily and seasonal patterns of temperature and moisture are more important for determining SOC turnover times than mean annual values. Furthermore, it remains unclear whether other variables like soil biodiversity also influence SOC turnover. However, MAT did have a major effect on the amount of active carbon, which increased by 3.4 t C ha^{-1} $°C^{-1}$ ($P < 0.001$). Since the turnover time of the active carbon pool was unaffected by MAT, this increase must have been due to the amount of carbon input as litter (above- and below-ground), which increased likewise with MAT (0.27 t C ha^{-1} yr^{-1} $°C^{-1}$, $P = 0.001$). On a continental scale, like in this study, MAT is positively related to the length of the growing season and to solar radiation (van Dijk et al., *submitted*). Since both growing season and solar radiation control net primary production and thereby litter input, climatic changes involving higher temperatures, longer growing seasons and higher radiation could increase net soil carbon sequestration. While C_{AP} increased significantly with mean annual temperature, the total amount of SOC did not. This suggests that the amount of non-active carbon is independent of mean annual temperature and litter input. Instead, the non-active carbon pool may primarily depend on soil texture, especially on the clay content (Telles et al. 2003). Thus, climate change could alter the amount of carbon stored in the active pool, but would leave the much larger non-active, recalcitrant carbon pool unaffected.

A key task for ecosystem carbon budgeting is the partitioning of heterotrophic and autotrophic soil respiration. Both fluxes involve major losses of carbon from ecosystems, but available partitioning methods are limited and mostly destructive. Thus, a new partitioning approach was developed, which involves the use of ^{14}C and the new two-pool model. This new approach, which can be applied to a wide range of different ecosystems, was successfully validated in three different girdling experiments. Using the new partitioning approach, both relative and absolute flux rates of heterotrophic and autotrophic soil respiration were calculated for six different forest stands and different times of year. Heterotrophic and autotrophic respiration varied considerably, both in time and among stands. The results indicate that heterotrophic and autotrophic soil respiration were related to latitude and tree species, but more stands need to be investigated to confirm these findings. Compared to most older approaches, the new ^{14}C partitioning approach has the advantage that

it is non-destructive and can therefore be applied repeatedly at the same locations in order to follow temporal changes in heterotrophic and autotrophic soil respiration. Apart from providing new insights into how terrestrial ecosystems function, the new partitioning approach can also help to improve global carbon cycle models, which include hetero- and autotrophic respiration as important variables.

With the presented new approaches for amount and turnover of active SOC and for CO_2 flux partitioning, I provide powerful and innovative tools for carbon cycle research. Both approaches can be applied to a wide range of ecosystems, from tundras to savannas, from agricultural fields to forests. They enable the separate investigation of active soil carbon (amount and turnover), heterotrophic and autotrophic soil respiration and the elucidation of factors controlling these variables. In this study, several questions of carbon cycle research could be answered, but also new questions were raised. As a next step, these questions ought to be tackled using the new approaches developed in this study, combined with other innovative approaches:

To elucidate the factors that control the highly variable turnover times observed, it would be a promising task to compare the new ^{14}C model with independent bottom-up models for SOC turnover, which take into account synergetic effects of different factors controlling SOC turnover and short-term variations of climatic variables like temperature and moisture. These investigations should concentrate on stands like Waldstein and Aubure*Picea*., which showed surprisingly different turnover times despite similarities in species composition and site conditions.

The new two-pool model overcomes some of the major deficiencies of older models and was successfully validated. Nevertheless, it can still be improved. The model assumes an exponential decay of fresh litter, which becomes part of the active carbon pool. However, decomposition studies suggest that litter decay slows down with time (Berg et al. 1996, Latter et al. 1998). A promising mathematical approach that can account for this effect is the "hockey stick" function, described by Feng and Li (2001). While the simple exponential decay function contains only one variable, the hockey stick function contains two to three. Therefore, more constraints for SOC turnover are required. One constraint could be decomposition studies performed in the field or in the lab. Also ^{13}C can serve as an additional constraint, when a vegetation shift has changed the ^{13}C content of carbon input into SOC. This phenomenon is well known for shifts from C3 to C4 plants, but also shifts from grassland or deciduous forest to evergreen forest (or vice versa) change $\delta^{13}C$ of litter input by approximately 3‰ ($\Delta\delta^{13}C$) (Hahn 2000). Another potential constraint may be ^{3}H (tritium).

Similar to ^{14}C, atmospheric ^{3}H contents increased rapidly during nuclear bomb tests in the 1950s and 1960s. Via rain, water uptake and litter, the ^{3}H enriched hydrogen has been transferred to plant and soil organic matter (Davis et al. 2002). While some organic hydrogen is in isotopic exchange with water, hydrogen directly bound to carbon atoms (as, e.g., in alkanes) is not exchangeable (Schimmelmann et al. 1999). Since the half-time of ^{3}H is only 12 years (compared to 5730 years for ^{14}C), the ^{3}H content of old, inactive organic matter should be close to zero. There seems to be no literature on this so far, but ^{3}H may in fact be a powerful, additional constraint for SOC turnover.

The ^{14}C approach has proven a promising tool for partitioning heterotrophic and autotrophic soil respiration. Nevertheless, some uncertainty remains about the ^{14}C content of true heterotrophically respired CO_2 in undisturbed stands. The new approach ought to be compared further with other methods for determining the ^{14}C content of heterotrophically respired CO_2 and for partitioning respiration fluxes. One approach would be to determine the ^{14}C content of heterotrophic, short-lived soil microbes and fungi, which should correspond to the ^{14}C content of the CO_2 they respire. Furthermore, it ought to be tested whether the ^{14}C content of heterotrophically respired CO_2 is constant or if it depends on temperature, moisture or time of year. The partitioning method was only applied to soil respiration. Since nearly all heterotrophic respiration occurs in the soil and all autotrophic respiration involves the loss of recently assimilated carbon, it should also be possible to apply the ^{14}C approach to total ecosystem respiration. In this case, the ^{14}C content of ecosystem respiration could be determined by the application of Keeling plots to canopy CO_2 (Buchmann and Ehleringer 1998, Pataki et al. 2003).

6 Abstract

One of the most controversial aspects of carbon cycle research is the potential of soils to serve as sinks for atmospheric CO_2, which is believed to drive global warming. In this study, major aspects of the soil carbon cycle, which determine soil carbon sequestration, and their potential responses to changes in climate and other environmental factors were elucidated and explained. These include amounts and turnover times of soil organic carbon (SOC), heterotrophic and autotrophic soil respiration and isotopic patterns (^{13}C, ^{14}C and ^{18}O) of soil CO_2 and soil respired CO_2.

A new model ("two-pool model") was developed, which uses the ^{14}C content of soil organic carbon (SOC) to calculate amount (C_{AP}) and turnover time (TT_{AP}) of the active soil carbon pool (chapter 2). Contrary to older ^{14}C turnover models, the new two-pool model focuses on the active component of soil carbon, as only the active pool can change its size significantly on short to intermediate time scales, a process involving carbon sequestration. The two-pool model overcomes major deficiencies of older models, particularly in respect to the ^{14}C content of carbon input to SOC and of carbon output from SOC. The model was successfully validated in incubation experiments and applied to 25 forest stands in Europe. Both C_{AP} and TT_{AP} varied by a factor of more than four, ranging from 11.6 to 55.7 t C ha^{-1} and from 4.5 to 18.3 years, respectively. TT_{AP} did not show significant relations with stand specific factors like latitude, mean annual temperature (MAT), annual rainfall, nitrogen deposition or stand age. In contrast, C_{AP} increased highly significantly with mean annual temperature (3.4 t C ha^{-1} $°C^{-1}$, $P < 0.001$). Likewise, measured litter input increased with MAT (0.27 t C ha^{-1} yr^{-1} $°C^{-1}$, $P = 0.001$). MAT is closely related to the length of the growing season and to solar radiation. These variables drive net primary production and thus litter production and can therefore explain the positive relationship between C_{AP} and MAT. As a consequence, climatic changes involving higher temperatures, longer growing seasons and higher solar radiation could enhance soil carbon sequestration. However, sequestration rates were simulated for three different forest soils by gradually increasing litter input or active pool turnover time by 50%, respectively, and the results clearly show that potential carbon sequestration rates are low compared to numbers discussed in the prevailing literature and decrease rapidly once litter input or turnover times stop increasing.

The potential of using ^{14}C contents of soil respired CO_2 to calculate the contributions of heterotrophic and autotrophic respiration to total soil respiration was experimentally assessed in the field (chapter 3). Respiration is the most important process causing carbon losses from

soils and ecosystems, and the partitioning of its heterotrophic and autotrophic components is of utmost importance to assess implications of environmental change on soil carbon cycling and sequestration. At three forest stands in Sweden and Germany, where autotrophic respiration had been strongly reduced by girdling, both flux rates and ^{14}C contents of soil respired CO_2 were measured in the summers of 2001 or 2002. At all stands, CO_2 flux rates were higher in the control plots, while the ^{14}C contents of respired CO_2 were higher in the girdled plots. This was expected and confirmed that heterotrophically respired carbon cycles more slowly through the forest ecosystem than autotrophically respired carbon. Data on flux rates and ^{14}C contents were used in two separate approaches to calculate the contributions of hetero- and autotrophic respiration to total soil respiration. Fractions of heterotrophic respiration ranged from 53 to 87% and values calculated by both approaches did not differ significantly from each other.

^{14}C contents of heterotrophically respired CO_2 were not only measured in the girdled plots, but also calculated by three different ^{14}C turnover models, including the new two-pool model (chapter 3); the respective ^{14}C values were then used for calculating the fractions of heterotrophic soil respiration. The aim was to assess the potential of using models for CO_2 flux partitioning. While the two older models gave lower ^{14}C values than measured in the girdled plots, the new two-pool model resulted in higher values. However, girdling may cause the ^{14}C content of CO_2 respired in the girdled plots to be lower than true heterotrophically respired CO_2 in undisturbed plots. This is because some roots may continue to respire young starch reserves in the girdled plots, dying fine roots may feed young carbon to heterotrophs and decreased root activity may decrease the decomposition of relatively old SOC (decreased "priming"). Heterotrophic respiration fractions calculated using the two older models were not defined (i.e., <0% or >100%). Heterotrophic respiration fractions calculated using the two-pool model were smaller compared to calculated fractions using the ^{14}C values measured in the girdled plots, but may be close to the true fractions of heterotrophic respiration in undisturbed plots due to the aforementioned girdling effects.

The new partitioning method was applied to soils of six non-girdled European forest stands using the two-pool model for calculating the ^{14}C content of heterotrophically respired CO_2 (chapter 4). Fractions of heterotrophic respiration ranged from 6 to 82% with a mean of 42%. Absolute CO_2 flux rates of heterotrophic respiration were high for northern stands and a beech stand, while autotrophic respiration rates were high for pine stands. Heterotrophic and autotrophic soil respiration could not be partitioned on limestone stands due to the dissolution

of ^{14}C free geogenic carbonates. The average fraction of soil respired CO_2 derived from carbonate dissolution was estimated to be about 3%.

Spatial and temporal patterns of ^{14}C, ^{13}C and ^{18}O contents of soil respired CO_2 and soil CO_2 were determined and explained for a variety of European forest stands, which formed a latitudinal gradient and included two age chronosequences (chapter 4). These isotopic patterns of soil CO_2 and soil respired CO_2 can provide information about the contributions of different processes to ecosystem fluxes. A large variability with both latitude and time of year was found for the ^{13}C content of soil respired CO_2. At all stands, ^{13}C contents were highest in summer, probably due to decreased water availability. ^{13}C contents of soil respired CO_2 determined by a Keeling plot using ^{13}C contents of soil CO_2 were lower than values determined by a simple chamber method. The Keeling plot method seems to systematically underestimate the ^{13}C content of soil respired CO_2 due to isotopic fractionation during diffusion of CO_2 that is produced within the soil. The ^{14}C content of soil respired CO_2 increased linearly with stand age ($P = 0.005$) at a spruce chronosequence in June/July, indicating an increasing fraction of heterotrophic respiration with stand age. Soil CO_2 in 5-10 cm depth was on average enriched in ^{18}O compared to CO_2 in isotopic equilibrium with rainwater by 0.4‰ ($\Delta\delta^{18}O$). This enrichment was mainly caused by the invasion of ^{18}O enriched atmospheric CO_2 into the soil.

7 References

Amundson, R. G., L. Stern, T. Baisden, and Y. Wang. 1998. The isotopic composition of soil and soil-respired CO_2. Geoderma **82**:83-114.

Baisden, W. T., R. Amundson, D. L. Brenner, A. C. Cook, C. Kendall, and J. W. Harden. 2002. A multiisotope C and N modeling analysis of soil organic matter turnover and transport as a function of soil depth in a California annual grassland soil chronosequence. Global Biogeochemical Cycles **16**:1135.

Berg, B., G. Ekbohm, M. B. Johansson, C. McClaugherty, F. Rutigliano, and A. V. DeSanto. 1996. Maximum decomposition limits of forest litter types: A synthesis. Canadian Journal of Botany-Revue Canadienne De Botanique **74**:659-672.

Boone, R. D., K. J. Nadelhoffer, J. D. Canary, and J. P. Kaye. 1998. Roots exert a strong influence on the temperature sensitivity of soil respiration. Nature **396**:570-572.

Bowden, R. D., K. J. Nadelhoffer, R. D. Boone, J. M. Melillo, and J. B. Garrison. 1993. Contributions of aboveground litter, belowground litter, and root respiration to total soil respiration in a temperature mixed hardwood forest. Canadian Journal of Forest Research-Revue Canadienne De Recherche Forestiere **23**:1402-1407.

Buchmann, N., and J. R. Ehleringer. 1998. CO_2 concentration profiles, and carbon and oxygen isotopes in C-3, and C-4 crop canopies. Agricultural and Forest Meteorology **89**:45-58.

Buchmann, N., J. R. Brooks, K. D. Rapp, and J. R. Ehleringer. 1996. Carbon isotope composition of C-4 grasses is influenced by light and water supply. Plant, Cell and Environment **19**:392-402.

Buchmann, N., W. Y. Kao, and J. Ehleringer. 1997. Influence of stand structure on carbon-13 of vegetation, soils, and canopy air within deciduous and evergreen forests in Utah, United States. Oecologia **110**:109-119.

Buchmann, N., V. Hahn, K. Sörgel, M. Andersson, M. Chauvat, M. F. Cotrufo, A. Richter, T. Persson, J.-A. Subke, S. Struwe, W. Wanek, V. Wolters, and B. Zeller. Soil carbon and nitrogen dynamics and soil biodiversity after girdling two spruce stands of different age in Germany. Global Change Biology, *in preparation*.

Cerling, T. E., and Y. Wang. 1996. Stable carbon and oxygen isotopes in soil CO_2 and soil carbonate: theory, practice, and application to some prairie soils of upper midwestern North America. Pages 113-131 *in* T. W. Boutton and S. Yamasaki, editors. Mass spetrometry in soils. Marcel Dekker, INC, New York.

Certini, G., G. Corti, A. Agnelli, and G. Sanesi. 2003. Carbon dioxide efflux and concentrations in two soils under temperate forests. Biology and Fertility of Soils **37**:39-46.

Chen, Q. Q., Y. M. Sun, C. D. Shen, S. L. Peng, W. X. Yi, Z. Li, and M. T. Jiang. 2002. Organic matter turnover rates and CO_2 flux from organic matter decomposition of mountain soil profiles in the subtropical area, south China. Catena **49**:217-229.

Craig, H. 1961. Isotopic variations in meteoric waters. Science **133**:1702-1703.

Davis, P. A., T. G. Kotzer, and W. J. G. Workman. 2002. Environmental tritium concentrations due to continuous atmospheric sources. Fusion Science and Technology **41**:453-457.

Dörr, H., and K. O. Münnich. 1986. Annual variations of the C-14 content of soil CO_2. Radiocarbon **28**:338-345.

Edwards, N. T., and P. Sollins. 1973. Continuous measurement of carbon-dioxide evolution from partitioned forest floor components. Ecology **54**:406-412.

Ekblad, A., and P. Högberg. 2001. Natural abundance of C-13 in CO_2 respired from forest soils reveals speed of link between tree photosynthesis and root respiration. Oecologia **127**:305-308.

Epron, D., L. Farque, E. Lucot, and P. M. Badot. 1999. Soil CO_2 efflux in a beech forest: the contribution of root respiration. Annals of Forest Science **56**:289-295.

Ewel, K. C., W. P. Cropper, Jr, and H. L. Gholz. 1987. Soil CO_2 evolution in Florida slash pine plantations. II. Importance of root respiration. Can. J. For. Res. **17**:330-333.

Farquhar, G. D., J. R. Ehleringer, and K. T. Hubick. 1989. Carbon isotope discrimination and photosynthesis. Annual Review of Plant Physiology and Plant Molecular Biology **40**:503-537.

Feng, Y. S., and X. M. Li. 2001. An analytical model of soil organic carbon dynamics based on a simple "hockey stick" function. Soil Science **166**:431-440.

Gansert, D. 1994. Root respiration and its importance for the carbon balance of beech saplings (*Fagus sylvatica* L.) in a montane beech forest. Plant and Soil **167**:109-119.

Gaudinski, J. B., S. E. Trumbore, E. A. Davidson, A. C. Cook, D. Markewitz, and D. D. Richter. 2001. The age of fine-root carbon in three forests of the eastern United States measured by radiocarbon. Oecologia **129**:420-429.

Gaudinski, J. B., S. E. Trumbore, E. A. Davidson, and S. H. Zheng. 2000. Soil carbon cycling in a temperate forest: radiocarbon-based estimates of residence times, sequestration rates and partitioning of fluxes. Biogeochemistry **51**:33-69.

Giardina, C. P., and M. G. Ryan. 2000. Evidence that decomposition rates of organic carbon in mineral soil do not vary with temperature. Nature **404**:858-861.

Gill, R. A., H. W. Polley, H. B. Johnson, L. J. Anderson, H. Maherali, and R. B. Jackson. 2002. Nonlinear grassland responses to past and future atmospheric CO_2. Nature **417**:279-282.

Gleixner, G., N. Poirier, R. Bol, and J. Balesdent. 2002. Molecular dynamics of organic matter in a cultivated soil. Organic Geochemistry **33**:357-366.

Hagedorn, F., D. Spinnler, M. Bundt, P. Blaser, and R. Siegwolf. 2003. The input and fate of new C in two forest soils under elevated CO_2. Global Change Biology **9**:862-872.

Hahn, V. 2000. δ^{13}C-Werte individueller Humus-Strukturbausteine als stabile Indikatoren des Streueintrags. Diploma thesis. University of Bayreuth.

Hanson, P. J., N. T. Edwards, C. T. Garten, and J. A. Andrews. 2000. Separating root and soil microbial contributions to soil respiration: A review of methods and observations. Biogeochemistry **48**:115-146.

Harkness, D. D., A. F. Harrison, and P. J. Bacon. 1986. The temporal distribution of "bomb" ^{14}C in a forest soil. Radiocarbon **28**:328-337.

Harrison, A. F., D. D. Harkness, A. P. Rowland, J. S. Garnett, and P. J. Bacon. 2000. Annual carbon and nitrogen fluxes in soils along the European forest transect, determined using ^{14}C-bomb. *in* E. D. Schulze, editor. Carbon and Nitrogen Cycling in European Forest Ecosystems. Springer, Heidelberg.

Hesterberg, R., and U. Siegenthaler. 1991. Production and stable isotopic composition of CO_2 in a soil near Bern, Switzerland. Tellus Series B-Chemical and Physical Meteorology **43**:197-205.

Högberg, P., and A. Ekblad. 1996. Substrate-induced respiration measured in situ in a C-3-plant ecosystem using additions of C-4-sucrose. Soil Biology & Biochemistry **28**:1131-1138.

Högberg, P., A. Nordgren, N. Buchmann, A. F. S. Taylor, A. Ekblad, M. N. Högberg, G. Nyberg, M. Ottosson-Löfvenius, and D. J. Read. 2001. Large-scale forest girdling drives soil respiration. Nature **411**:789-792.

Horwath, W. R., K. S. Pregitzer, and E. A. Paul. 1994. C-14 allocation in tree soil systems. Tree Physiology **14**:1163-1176.

Hsieh, Y. P. 1993. Radiocarbon signatures of turnover rates in active soil organic carbon pools. Soil Science Society of America Journal **57**:1020-1022.

IAEA/WMO. 2001. Global Network of Isotopes in Precipitation. The GNIP Database. Accessible at: http://isohis.iaea.org

IPCC. 2001. Climate change 2001. The scientific basis. Contribution of working group I to the Third Assessment Report of the IPPC. Cambridge University Press, Cambridge.

Janssens, I. A., A. Freibauer, P. Ciais, P. Smith, G. J. Nabuurs, G. Folberth, B. Schlamadinger, R. W. A. Hutjes, R. Ceulemans, E. D. Schulze, R. Valentini, and A. J. Dolman. 2003a. Europe's terrestrial biosphere absorbs 7 to 12% of European anthropogenic CO_2 emissions. Science **300**:1538-1542.

Janssens, I. A., S. Dore, D. Epron, H. Lankreijer, N. Buchmann, B. Longdoz, J. Brossaud, and L. Montagnani. 2003b. Climatic influences on seasonal and spatial differences in soil CO_2 efflux. Pages 233-253 *in* Fluxes Of Carbon, Water And Energy Of European Forests.

Jobbagy, E. G., and R. B. Jackson. 2000. The vertical distribution of soil organic carbon and its relation to climate and vegetation. Ecological Applications **10**:423-436.

Jordan, A., and W. A. Brand. 2001. Technical report. *in* T. Sasaki, editor. Eleventh WMO/IAEA Meeting of experts on carbon dioxide concentration and related tracer measurement techniques. World Meteorological Organization, Tokyo.

Keeling, C. D. 1958. The concentration and isotopic abundances of atmospheric carbon dioxide in rural areas. Geochimica et Cosmochimica Acta **13**:322-334.

Koarashi, J., H. Amano, M. Andoh, T. Iida, and J. Moriizumi. 2002. Estimation of (CO_2)-C-14 flux at soil-atmosphere interface and distribution of C-14 in forest ecosystem. Journal of Environmental Radioactivity **60**:249-261.

Kromer, B., S. W. Manning, P. I. Kuniholm, M. W. Newton, M. Spurk, and I. Levin. 2001. Regional (CO_2)-C-14 offsets in the troposphere: Magnitude, mechanisms, and consequences. Science **294**:2529-2532.

Krull, E. S., and J. O. Skjemstad. 2003. delta C-13 and delta N-15 profiles in C-14-dated Oxisol and Vertisols as a function of soil chemistry and mineralogy. Geoderma **112**:1-29.

Kuzyakov, Y., and W. Cheng. 2001. Photosynthesis controls of rhizosphere respiration and organic matter decomposition. Soil Biology & Biochemistry **33**:1915-1925.

Kuzyakov, Y., J. K. Friedel, and K. Stahr. 2000. Review of mechanisms and quantification of priming effects. Soil Biology & Biochemistry **32**:1485-1498.

Langendörfer, U., M. Cuntz, P. Ciais, P. Peylin, T. Bariac, I. Milyukova, O. Kolle, T. Naegler, and I. Levin. 2002. Modelling of biospheric CO_2 gross fluxes via oxygen isotopes in a spruce forest canopy: a Rn-222 calibrated box model approach. Tellus Series B-Chemical and Physical Meteorology **54**:476-496.

Latter, P. M., G. Howson, D. M. Howard, and W. A. Scott. 1998. Long-term study of litter decomposition on a pennine neat bog - which regression. Oecologia **113**:94-103.

Levin, I., and V. Hesshaimer. 2000. Radiocarbon - A unique tracer of global carbon cycle dynamics. Radiocarbon **42**:69-80.

Levin, I., and B. Kromer. 1997. Twenty years of atmospheric $^{14}CO_2$ observations at Schauinsland Station, Germany. Radiocarbon **39**:205-218.

Levin, I., B. Kromer, H. Schochfischer, M. Bruns, M. Munnich, D. Berdau, J. C. Vogel, and K. O. Munnich. 1985. 25 years of tropospheric C-14 observations in Central-Europe. Radiocarbon **27**:1-19.

Li, T. Y., S. J. Wang, and L. P. Zheng. 2002. Comparative study on CO_2 sources in soil developed on carbonate rock and non-carbonate rock in Central Guizhou. Science in China Series D-Earth Sciences **45**:673-679.

Lin, G. H., J. R. Ehleringer, P. T. Rygiewicz, M. G. Johnson, and D. T. Tingey. 1999. Elevated CO_2 and temperature impacts on different components of soil CO_2 efflux in Douglas-fir terracosms. Global Change Biology **5**:157-168.

Magid, J., G. Cadisch, and K. E. Giller. 2002. Short and medium term plant litter decomposition in a tropical Ultisol elucidated by physical fractionation in a dual C-13 and C-14 isotope study. Soil Biology & Biochemistry **34**:1273-1281.

Miller, J. B., D. Yakir, J. W. C. White, and P. P. Tans. 1999. Measurement of O-18/O-16 in the soil-atmosphere CO_2 flux. Global Biogeochemical Cycles **13**:761-774.

Mook, W. G., and J. van der Plicht. 1999. Reporting C-14 activities and concentrations. Radiocarbon **41**:227-239.

Mortazavi, B., and J. P. Chanton. 2002. Carbon isotopic discrimination and control of nighttime canopy delta O-18-CO_2 in a pine forest in the southeastern United States. Global Biogeochemical Cycles **16**:1008.

O'Brien, B. J., and J. D. Stout. 1978. Movement and turnover of soil organic matter as indicated by carbon isotope measurements. Soil Biology & Biochemistry **10**:309-317.

Pataki, D. E., J. R. Ehleringer, L. B. Flanagan, D. Yakir, D. R. Bowling, C. J. Still, N. Buchmann, J. O. Kaplan, and J. A. Berry. 2003. The application and interpretation of Keeling plots in terrestrial carbon cycle research. Global Biogeochemical Cycles **17**:art. no.-1022.

Persson, T., H. van Oene, A. F. Harrison, P. S. Karlsson, J. Cerny, M.-M. Couteaux, E. Dambrine, P. Högberg, A. Kjoller, G. Matteucci, A. Rudebeck, E. D. Schulze, and T. Paces. 2000. Experimental sites in the NIPHYS/CANIF project. *in* E. D. Schulze, editor. Carbon and Nitrogen Cycling in European Forest Ecosystems. Springer, Heidelberg.

Pessenda, L. C. R., S. E. M. Gouveia, and R. Aravena. 2001. Radiocarbon dating of total soil organic matter and humin fraction and its comparison with C-14 ages of fossil charcoal. Radiocarbon **43**:595-601.

Plamboeck, A. H., H. Grip, and U. Nygren. 1999. A hydrological tracer study of water uptake depth in a Scots pine forest under two different water regimes. Oecologia **119**:452-460.

Poulton, P. R., E. Pye, P. R. Hargreaves, and D. S. Jenkinson. 2003. Accumulation of carbon and nitrogen by old arable land reverting to woodland. Global Change Biology **9**:942-955.

Powers, J. S., and W. H. Schlesinger. 2002. Geographic and vertical patterns of stable carbon isotopes in tropical rain forest soils of Costa Rica. Geoderma **109**:141-160.

Raich, J. W., and W. H. Schlesinger. 1992. The global carbon-dioxide flux in soil respiration and its relationship to vegetation and climate. Tellus Series B-Chemical and Physical Meteorology **44**:81-99.

Randerson, J. T., I. G. Enting, E. A. G. Schuur, K. Caldeira, and I. Y. Fung. 2002. Seasonal and latitudinal variability of troposphere Delta(CO_2)-C-14: Post bomb contributions from fossil fuels, oceans, the stratosphere, and the terrestrial biosphere. Global Biogeochemical Cycles **16**:art. no.-1112.

Riley, W. J., C. J. Still, M. S. Torn, and J. A. Berry. 2002. A mechanistic model of (H_2O)-O-18 and (COO)-O-18 fluxes between ecosystems and the atmosphere: Model description and sensitivity analyses. Global Biogeochemical Cycles **16**:1095.

Rom, W., C. A. M. Brenninkmeijer, C. B. Ramsey, W. Kutschera, A. Priller, S. Puchegger, T. Rockmann, and P. Steier. 2000. Methodological aspects of atmospheric (CO)-C-14 measurements with AMS. Nuclear Instruments & Methods in Physics Research, Section B: Beam Interactions with Materials and Atoms **172**:530-536.

Sanderman, J., R. G. Amundson, and D. D. Baldocchi. 2003. Application of eddy covariance measurements to the temperature dependence of soil organic matter mean residence time. Global Biogeochemical Cycles **17**:art. no.-1061.

Scarascia-Mugnozza, G., G. A. Bauer, H. Persson, G. Matteucci, and A. Masci. 2000. Tree biomass, growth and nutrient pools. Carbon And Nitrogen Cycling In European Forest Ecosystems **142**:49-62.

Schimmelmann, A., M. D. Lewan, and R. P. Wintsch. 1999. D/H isotope ratios of kerogen, bitumen, oil, and water in hydrous pyrolysis of source rocks containing kerogen types I, II, IIS, and III. Geochimica et Cosmochimica Acta **63**:3751-3766.

Schlesinger, W. H. 1997. Biogeochemistry, an analysis of global change. Academic Press, San Diego, USA.

Schlesinger, W. H., and J. Lichter. 2001. Limited carbon storage in soil and litter of experimental forest plots under increased atmospheric CO_2. Nature **411**:466-469.

Schulze, E. D., P. Högberg, H. van Oene, H. Persson, A. F. Harrison, D. J. Read, A. Kjöller, and G. Matteucci. 2000. Interactions between the carbon and nitrogen cycle and the role of biodiversity: A synopsis of a study along a North-South transect through Europe. Pages 257-275 *in* E. D. Schulze, editor. Carbon And Nitrogen Cycling In European Forest Ecosystems.

Schweizer, M., J. Fear, and G. Cadisch. 1999. Isotopic (C-13) fractionation during plant residue decomposition and its implications for soil organic matter studies. Rapid Communications in Mass Spectrometry **13**:1284-1290.

Sleutel, S., S. De Neve, and G. Hofman. 2003. Estimates of carbon stock changes in Belgian cropland. Soil Use and Management **19**:166-171.

Stern, L. A., R. Amundson, and W. T. Baisden. 2001. Influence of soils on oxygen isotope ratio of atmospheric CO_2. Global Biogeochemical Cycles **15**:753-759.

Strömgren, M. 2001. Soil-surface CO_2 flux and growth in a boreal Norway spruce stand. Effects of soil warming and nutrition. Acta Universitatis Agriculturae Sueciae, Silvestria 220. Dissertation thesis.

Stuiver, M., and H.A. Polach 1977. Discussion: Reporting of ^{14}C data. Radiocarbon **19**:355-363.

Stuiver, M., and P. D. Quay. 1981. Atmospheric C-14 changes resulting from fossil-fuel CO_2 release and cosmic-ray flux variability. Earth and Planetary Science Letters **53**:349-362.

Subke, J.-A., V. Hahn, G. Battipaglia, S. Linder, N. Buchmann, and M. F. Cotrufo. Surprising interactions between needle litter decomposition and rhizosphere activity. Oecologia, *in review*.

Swinnen, J., J. A. Vanveen, and R. Merckx. 1994. Rhizosphere carbon fluxes in field-grown spring wheat - model- calculations based on C-14 partitioning after pulse-labeling. Soil Biology & Biochemistry **26**:171-182.

Tans, P. P. 1981. A compilation of bomb ^{14}C data for use in global carbon model calculation. Pages 131-137 *in* B. Bolin, editor. Carbon Cycle Modelling. John Wiley.

Tans, P. P. 1998. Oxygen Isotopic Equilibrium Between Carbon Dioxide and Water in Soils. Tellus Series B-Chemical and Physical Meteorology **50**:163-178.

Tegen, I., and H. Dörr. 1996. C-14 measurements of soil organic matter, soil CO_2 and dissolved organic carbon (1987-1992). Radiocarbon **38**:247-251.

Telles, E. D. C., P. B. de Camargo, L. A. Martinelli, S. E. Trumbore, E. S. da Costa, J. Santos, N. Higuchi, and R. C. Oliveira. 2003. Influence of soil texture on carbon dynamics and storage potential in tropical forest soils of Amazonia. Global Biogeochemical Cycles **17**:1040.

Thierron, V., and H. Laudelout. 1996. Contribution of root respiration to total CO_2 efflux from the soil of a deciduous forest. Canadian Journal of Forest Research-Revue Canadienne De Recherche Forestiere **26**:1142-1148.

Tierney, G. L., and T. J. Fahey. 2002. Fine root turnover in a northern hardwood forest: a direct comparison of the radiocarbon and minirhizotron methods. Canadian Journal of Forest Research-Journal Canadien de la Recherche Forestiere **32**:1692-1697.

Torn, M. S., A. G. Lapenis, A. Timofeev, M. L. Fischer, B. V. Babikov, and J. W. Harden. 2002. Organic carbon and carbon isotopes in modern and 100-year-old- soil archives of the Russian steppe. Global Change Biology **8**:941-953.

Trumbore, S. 2000. Age of soil organic matter and soil respiration: Radiocarbon constraints on belowground C dynamics. Ecological Applications **10**:399-411.

Trumbore, S. E., O. A. Chadwick, and R. Amundson. 1996. Rapid exchange between soil carbon and atmospheric carbon dioxide driven by temperature change. Science **272**:393-396.

Trumbore, S. E., J. S. Vogel, and J. R. Southon. 1989. AMS ^{14}C measurements of fractionated soil organic matter: an approach to deciphering the soil carbon cycle. Radiocarbon **31**:664-654.

Trumbore, S. E., and S. H. Zheng. 1996. Comparison of fractionation methods for soil organic matter C-14 analysis. Radiocarbon **38**:219-229.

van Dijk, A. I. J. M., A. J. Dolman, and E. D. Schulze. Radiation, temperature and leaf area explain most variation in net ecosystem exchange among European forests. Global Change Biology, *submitted*.

Wang, Y., R. Amundson, and X. F. Niu. 2000. Seasonal and altitudinal variation in decomposition of soil organic matter inferred from radiocarbon measurements of soil CO_2 flux. Global Biogeochemical Cycles **14**:199-211.

Wang, Y., R. Amundson, and S. Trumbore. 1999. The impact of land use change on C turnover in soils. Global Biogeochemical Cycles **13**:47-57.

Wang, Y., R. Amundson, and S. E. Trumbore. 1996. Radiocarbon dating of soil organic matter. Quaternary Research **45**:282-288.

Wang, Y., and Y. P. Hsieh. 2002. Uncertainties and novel prospects in the study of the soil carbon dynamics. Chemosphere **49**:791-804.

Werner, R. A., and W. A. Brand. 2001. Referencing strategies and techniques in stable isotope ratio analysis. Rapid Communications in Mass Spectrometry **15**:501-519.

Yakir, D., and L. D. L. Sternberg. 2000. The use of stable isotopes to study ecosystem gas exchange. Oecologia **123**:297-311.

Yakir, D., and X. F. Wang. 1996. Fluxes of CO_2 and water between terrestrial vegetation and the atmosphere estimated from isotope measurements. Nature **380**:515-517.

8 Acknowledgements

Many people were involved in enabling the presented research. In particular, I want to thank the following persons:

Doug Harkness, **Tony Harrison** and **Phil Rowland** for providing ^{14}C data of SOC

Ingeborg Levin for providing ^{14}C data of atmospheric CO_2

Susan Trumbore for inspiring discussions about the world of ^{14}C

Peter Högberg for scientific cooperation and for access to his girdling stand Åheden*Pinus*

Anders Nordgren for supplying soil samples from the girdling stand Åheden*Pinus*

Armin Jordan for CO_2 mixing ratio measurements

Willi Brand, **Roland Werner, Heike Geilmann** and **Michael Rothe** for ^{13}C measurements

Michael Rässler, Ines Hilke and **Sandra Matthaei** for element analyses

Axel Steinhof and **Melanie Altenburg** for ^{14}C sample processing

Waldemar Ziegler for technical assistance in the design of field instruments

Karin Sörgel, **Dirk Sachse**, **Wolfgang Falk**, **Iris Kuhlmann**, **Joachim Janda**, **Michael Patecki**, **Frank Bäse**, **Lina Mercado, Juliane Anders** and **Karin Zuber** for their technical assistance in the field and in the lab

Anouk Janssen for conducting the incubation experiments

Gerd Gleixner, **Alexander Knohl**, **Martina Mund**, **Christian Wirth**, **Astrid Søe**, **Jens Schumacher**, **Claudia Czimczik**, **Ansgar Kahmen**, **Marcus Schumacher**, **Anna Ekberg** and **Manuel Gloor** for scientific discussions and inspirations

Annett Börner for helping with layout and design

The **computer team** and **administration** of the Max Planck Institute for their support

Ebba Hahn and **Gerhard Hahn** for their great support

Thanks to everyone I forgot.

Special thanks to my advisors:

Ernst-Detlef Schulze for inspiring discussions and his motivating enthusiasm

Thomas Scholten for the cooperation for my graduation and his advice on the dissertation

Most of all, my thanks go to **Nina Buchmann** for providing the opportunity to do this research. She was an excellent advisor and readily supported the realization of my ideas and activities.

9 Appendix

Appendix 1. Conversion of $\Delta^{14}C$ into pM, and of pM into $\Delta^{14}C$ for the years 1996[A] and 2002[B]. $\Delta^{14}C$ values are generally given for a defined year. Contrary to pM, $\Delta^{14}C$ of an individual substance (e.g., a sample of soil organic carbon or CO_2) changes with time. The conversion equation is given below.

$\Delta^{14}C$ (‰)	pM (%)[A]	pM (%)[B]	pM (%)	$\Delta^{14}C$ (‰)[A]	$\Delta^{14}C$ (‰)[B]
-55	95.0	95.1	95.0	-55	-56
-50	95.5	95.6	95.5	-50	-51
-45	96.0	96.1	96.0	-45	-46
-40	96.5	96.6	96.5	-40	-41
-35	97.0	97.1	97.0	-35	-36
-30	97.5	97.6	97.5	-30	-31
-25	98.0	98.1	98.0	-25	-26
-20	98.5	98.6	98.5	-20	-21
-15	99.0	99.1	99.0	-15	-16
-10	99.6	99.6	99.5	-11	-11
-5	100.1	100.1	100.0	-6	-6
0	100.6	100.6	100.5	-1	-1
5	101.1	101.1	101.0	4	4
10	101.6	101.6	101.5	9	9
15	102.1	102.1	102.0	14	14
20	102.6	102.6	102.5	19	19
25	103.1	103.1	103.0	24	24
30	103.6	103.6	103.5	29	29
35	104.1	104.2	104.0	34	33
40	104.6	104.7	104.5	39	38
45	105.1	105.2	105.0	44	43
50	105.6	105.7	105.5	49	48
55	106.1	106.2	106.0	54	53
60	106.6	106.7	106.5	59	58
65	107.1	107.2	107.0	64	63
70	107.6	107.7	107.5	69	68
75	108.1	108.2	108.0	74	73
80	108.6	108.7	108.5	79	78
85	109.1	109.2	109.0	84	83
90	109.6	109.7	109.5	89	88
95	110.1	110.2	110.0	94	93
100	110.6	110.7	110.5	99	98

A = for the year 1996
B = for the year 2002

$$\Delta^{14}C = \left[\frac{pM}{100} \times \exp\left(-\frac{Y-1950}{8267}\right) - 1\right] \times 1000‰,$$

where Y is the year of interest.

Appendix 1 (continuation).

$\Delta^{14}C$ (‰)	pM (%)[A]	pM (%)[B]	pM (%)	$\Delta^{14}C$ (‰)[A]	$\Delta^{14}C$ (‰)[B]
105	111.1	111.2	111.0	104	103
110	111.6	111.7	111.5	109	108
115	112.1	112.2	112.0	114	113
120	112.6	112.7	112.5	119	118
125	113.1	113.2	113.0	124	123
130	113.6	113.7	113.5	129	128
135	114.1	114.2	114.0	134	133
140	114.6	114.7	114.5	139	138
145	115.1	115.2	115.0	144	143
150	115.6	115.7	115.5	149	148
155	116.1	116.2	116.0	154	153
160	116.6	116.7	116.5	159	158
165	117.2	117.2	117.0	164	163
170	117.7	117.7	117.5	168	168
175	118.2	118.2	118.0	173	173
180	118.7	118.7	118.5	178	178
185	119.2	119.2	119.0	183	183
190	119.7	119.8	119.5	188	188
195	120.2	120.3	120.0	193	192
200	120.7	120.8	120.5	198	197
205	121.2	121.3	121.0	203	202
210	121.7	121.8	121.5	208	207
215	122.2	122.3	122.0	213	212
220	122.7	122.8	122.5	218	217
225	123.2	123.3	123.0	223	222
230	123.7	123.8	123.5	228	227
235	124.2	124.3	124.0	233	232
240	124.7	124.8	124.5	238	237
245	125.2	125.3	125.0	243	242

A = for the year 1996
B = for the year 2002

Appendix 2. ^{14}C contents ($\Delta^{14}C$ and pM) of atmospheric CO_2 measured at atmospheric observation stations in Europe and derived from tree ring ^{14}C measurements. $\Delta^{14}C$ values are given for the referred year. The pM value of an individual substance (e.g., CO_2 collected in a specific year) does not change with time.

Year	$\Delta^{14}C$ (‰)	pM (%)
1510	11	95.8
1530	12	96.1
1550	9	96.2
1570	7	96.1
1590	4	96.2
1610	-3	95.7
1630	-4	95.8
1650	6	97.0
1670	10	97.6
1690	14	98.3
1710	18	98.8
1730	11	98.4
1750	5	98.1
1770	0	97.8
1790	-7	97.4
1810	2	98.5
1830	4	98.9
1850	-1	98.7
1870	-5	98.6
1890	-2	99.1
1910	-7	98.8
1930	-14	98.4
1950	-25	97.5
1951	-25	97.5
1952	-25	97.5
1953	-24	97.6
1954	-21	97.9
1955	-8	99.2
1956	27	102.7
1957	73	107.4
1958	140	114.1
1959	228	122.9
1960	212	121.4
1961	222	122.3
1962	359	136.0
1963	718	172.1
1964	836	183.9
1965	756	175.9
1966	692	169.5
1967	624	162.7
1968	565	156.8
1969	545	154.9
1970	529	153.3
1971	499	150.3
1972	466	147.0
1973	419	142.3
1974	401	140.5
1975	370	137.4
1976	353	135.7
1977	334	133.8
1978	326	133.0
1979	296	130.0
1980	265	126.9
1981	257	126.1
1982	238	124.3
1983	224	122.9
1984	209	121.4
1985	201	120.6
1986	189	119.5
1987	181	118.6
1988	171	117.7
1989	164	116.9
1990	152	115.7
1991	141	114.7
1992	136	114.1
1993	126	113.2
1994	121	112.7
1995	116	112.2
1996	107	111.3
1997	102	110.8
1998	99	110.5
1999	95	110.2
2000	88	109.5
2001	82	108.8
2002	75	108.1

^{14}C data from 1510 to 1889 were taken from *Stuiver, M. and T. F. Braziunas. 1993. Sun, ocean, climate, and atmospheric $^{14}CO_2$: An evaluation of causal and spectral relationships. The Holocene 3: 289-305*, and from *Stuiver, M., P. J. Reimer and T. F. Braziunas. 1998. High-precision radiocarbon age calibration for terrestrial and marine samples. Radiocarbon 40: 1127-1151*. For the period from 1890 until today, see chapter 2.